UNIVERSITÀ
DEGLI STUDI
FIRENZE

DOTTORATO DI RICERCA IN
Scienze Agrarie ed Ambientali

CICLO *XXXII*

COORDINATORE Prof. Giacomo Pietramellara

Generation of bio-compounds from microbial catalysts fueled by CO2 and electrons, with potential for the production of biofuels and compounds of interest.

Settore Scientifico Disciplinare AGR/16

Dottorando
Dott. *La Cava Eugenio*

Tutore
Prof. *De Philippis Roberto*

Coordinatore
Prof. *Pietramellara Giacomo*

Anni 2017/2021

UNIVERSITÀ
DEGLI STUDI
FIRENZE

DAGRI Dipartimento di Scienze e
Tecnologie Agrarie, Alimentari
Ambientali e Forestali

Corso di Dottorato in Scienze Agrarie e
Ambientali
Ciclo XXXII

Generation of bio-compounds from microbial catalysts fueled by CO_2 and electrons, with potential for the production of biofuels and compounds of interest.

Candidate

Eugenio La Cava (ID number DT30006)

Thesis Advisors

Prof. Roberto De Philippis

Dr. Stefano Mocali

Academic Year 2019/2020

Coordinatore:

Prof. PIETRAMELLARA GIACOMO

Thesis not yet defended

Reviewers:

Prof. Alessio Mengoni

Prof. Mauro Maione

Generation of bio-compounds from microbial catalysts fueled by CO_2 and electrons, with potential for the production of biofuels and compounds of interest.

PhD Thesis. University of Florence

This thesis has been typeset by LaTeX and the UniFiTh class.

Author's email: eugenio.lacava@unifi.it

Dedicated to

my daughter Emily and to my family whole.

Abstract

This thesis is dealing with my work in the field of microbial electrochemistry of relevant microbial strains applied to microbial electrolytic cells. It consists of two main topics: the electrochemical characterization of the novel CO_2 reduction reaction in the electroactive model bacterium *Shewanella oneidensis* MR-1 and the electrochemical characterization of strain 42OL of the Purple Non Sulfur Bacteria *Rhodopseudomonas palustris*.

During the time I was in Japan at the University of Tokyo, I explored the possibility of carbon fixation by *Shewanella oneidensis* MR-1 model microbe for anodic extracellular electron transfer process. The results showed that the current consumed by the strain was indeed increasing upon bubbling with carbon dioxide, while when administering argon gas did not increase the current uptake. While I was not able to identify the product of carbon fixation at the time, a successive search in the literature revealed that Shewanella is able to produce formate in experimental conditions similar to those that I used.

At University of Florence and CREA, I carried out the electrochemical characterization of a strain of Purple Non Sulfur Bacteria, *Rhodopseudomonas palustris* 42OL and explored the possibility of single culture electrochemically driven biological nitrogen fixation. The results are quite surprising, in fact, *Rps. palustris* 42OL is indeed electroactive in both anodic and cathodic modes, and in addition to that it exhibits a noteworthy current uptake in the cathodic mode while the electrochemical cell medium is bubbled with high purity nitrogen gas. Scanning Electron Microscope micrographies are also showing that *Rps. palustris* 42OL is directly attached to the Working Electrode and possibly forms subcellular structures like nanowires, thereby meaning that the mechanism of electron transfer to the electrode is also of direct type.

Contents

Chapter 1

Introduction

1.1 Extracellular Electron Transport (EET) in the microbial world

1.1.1 Short history of Extracellular Electron Transport

In the second half of the 1980s, two gram-negative strains of different species (*Geobacter metallireducens* GS-15 and *Shewanella oneidensis* MR-1) were isolated and it was discovered that they possessed the ability of degrading organic matter and grow under anaerobic condition in the presence of manganese or iron (hydr)oxide minerals [64, 49, 39]. These and other microbes, belonging to different species but possessing similar capabilities are known as dissimilatory metal reducing bacteria (or DMRB) and for several years the mechanisms by which the metal reduction was taking place remained elusive until their genomes were sequenced and analyzed (in 2002 for *Shewanella* and 2009 for *Geobacter*), although some preliminary clues were found earlier for *Geobacter* spp. [2, 26]. From there on, the arsenal of molecular microscopy and biochemical techniques was greatly expanded with every year and the mechanism of Extracellular Electron Transport (EET) was elucidated for these two microbes and generalized for the rest of gram-negative microbes.

It was discovered, in different moments, that the molecular mechanisms underlying the Extracellular Electron Transport in *Shewanella oneidensis* MR-1 and Geobacter were mediated, in certain cases, by different and unrelated structures.

This is the case of electron conducting pili in *Geobacter* spp. [38, 63] and nanowires of *S. oneidensis* MR-1 [35] that rely on different molecular mechanism to transfer electrons on µm-scale distances. In other cases, the molecular mechanisms were found to be similar [54] while the proteins involved in EET chain in both microbes are often only partially equivalent in terms of function, number, sequences. In addition, the heme groups within each of these can vary significantly. It is common thinking that EET is an example of convergent evolution because of the ample diffusion of this behavior, the distances in the relatedness of genetic sequences involved in this phenomenon, and the differences in mechanism among the kingdoms of bacteria and archaea and within the bacterial kingdom itself[40].

1.1.2 Types of EET

EET modes are not all the same and their performance can vary according to different limitations. There are three types of EET: two direct EET, with both long range and short range carried out by conductive pili and nanowires or c-type cytochromes respectively, and one indirect EET that depends on the diffusion of redox molecules. Moreover, the performances of the three are in the following order: *Geobacter*'s pili and *Shewanella*'s nanowires have comparable electron transfer rates for in vitro conditions, up to $10^9 e^-$/s [63, 48, 32] while the indirect electron transfer is limited by the diffusion coefficient in the medium and the concentration of the redox molecule acting as an electron shuttle and it is therefore slower.

1.1.3 Mechanisms of electron conduction

For what concerns gram-negative EET-active model microbes, the mechanisms of electron conduction of each EET mode are almost completely elucidated and their physiologic electron transport rate constants have been measured and calculated with good accordance between experimental and theoretical measurements [63, 48, 32]. The second part of this statement is valid if one considers only the electron transfer rates of the EET chain and not the limitations due to metabolism and electron acceptor/donor availability that a cell might be subjected to. When *Shewanella* is put under physiological conditions, the electron transfer rate per single Outer Membrane

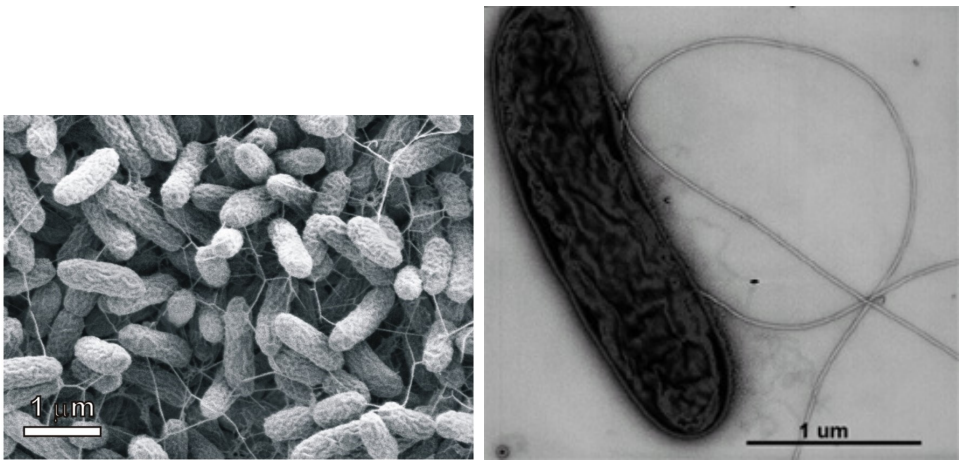

(a) **(b)**

Figure 1.1. (a): *Shewanella oneidensis* MR-1 biofilm with nanowires, reproduced from "Shewanella oneidensis MR-1 bacterial nanowires exhibit p-type, tunable electronic behavior. Nano Letters, 2013, 13, 2407-2411" [35] (b): *Geobacter metallireducens* cell with flagella and pili, reproduced from "Geobacter metallireducens accesses insoluble Fe(iii) oxide by chemotaxis. Nature, Nature Publishing Group, 2002, 416, 767-769" [12]

C-type Cytochrome OMCC complex is not the reported one in 1.1.2, instead it was determined experimentally a number around 330 $e^{-}\,\mathrm{s}^{-1}$ [53], that is several orders of magnitude lower. This is due to several reasons, the main one being probably some rate-limiting reaction inside the cell, because it was demonstrated by Okamoto et al. in [53] that the electron transfer rate of a Mtr-CAB complex immobilized in a proteoliposome is at least three times faster than the outer membrane in vivo condition one[53].

Another limiting factor that should be considered and that is not yet completely understood is the coupling of exportation, trough membranes, of the same equivalents of electrons in cation species (mainly protons). If the mechanism and structures of this phenomenon are known for the cytoplasmic membrane, it is not the case for the outer membrane even in the well-known gram-negative model microbe *Shewanella oneidensis* MR-1 [53]. It was hypothesized by Okamoto et al. that, due to the fact that there was no accumulation of an excess of protons in the periplasm in EET mode for *Shewanella*'s cells, a route for coupled proton/electron transport must exist

in this microbe [53, 73].

A further interesting fact is that both in *Shewanella* [55, 54] and *Geobacter* [56, 45, 54] riboflavin and other structurally similar redox-active molecules can work as a cofactor of OMCc (Outer Membrane C-type cytochromes) enhancing in a more or less evident manner the electron transfer rates [72].

If we consider all these factors together, we can conclude that EET rate is mainly limited by cell metabolism.

1.2 Importance of the research

Microbial electrosynthesis is a relatively recent research topic derived from the more general microbial fuel cell (MFC) field. A quick metric analysis on iCite (icite.od.nih.gov) shows that it has attracted interest in the last five years with a peak of over 30 publications in 2015 and about half of this number for the previous and following year. At the time of writing (08/2021), for the period 2005-2021, if one considers the last ten years interval (2011-2021), it is evident the increase of the research interest of the topic with the number of publications increasing almost every year until 2016. The average number of citations for the overall period is 13.44, with the latest years (2017-2021) well over 20 articles per year, meaning that this topic is alive and actively researched. In a more recent search on Google Scholar, we discovered a significant discrepancy in the number of available papers on the subject with a difference of one order of magnitude in the period 2010-2021 ($\approx$ 6450 vs 267 papers). This difference can be explained as iCite is basing its metrics on Pubmed's search engine, which is highly specialized in the medical field, while Google Scholar has a much broader spectrum of searched fields.

To further explain the importance of this research topic, we need to define its scope and meaning: in their recent paper, Shröder *et al.* [66] propose a new classification of the subjects in question. They start with the topic "bioelectrochemistry", subdivided in microbial, enzyme and DNA/protein electrochemistry subcategories. The microbial subcategory contains a sub-sub-category "Microbial electrocatalysis" that in turn includes the "Microbial electrosynthesis" topic.

After defining the scope of this topic, one might think that its importance is

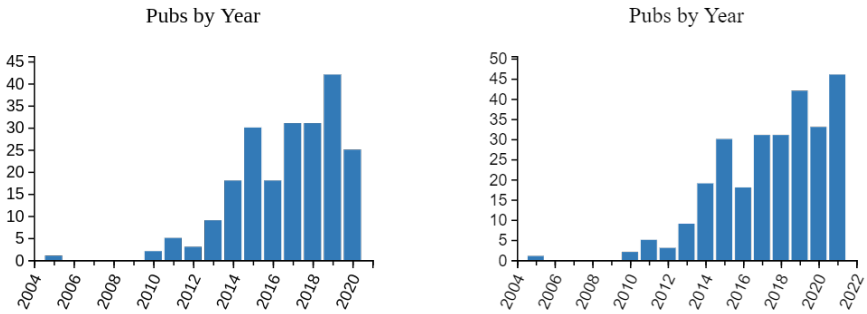

(a) **(b)**

Figure 1.2. (a): number of publications per year in the field of microbial electrosynthesis until 2020 (b): number of publications per year updated at 08/2021 (source: icite.od.nih.gov)

limited because of its high specialization, however, it is not only our belief that applications in this field have high potential in terms of revenue and environmental impact [77].

1.2.1 Applications of microbial electrosynthesis

Anodic (oxidative) and cathodic (reductive) bio-(photo-)electrochemical processes like microbial electrosynthesis and microbial electrolysis, have many useful applications, spacing from the synthesis of simple molecules like organic acids (formic or acetic)[20, 29, 51] or gases (methane in-primis) [42, 78, 34] to the more complex ones like polyhydroxybutyrate [61], other polyhydroxyalkanoates and other complex molecules. In addition, with the help of synthetic biology and metabolic pathways from different bacterial and nonbacterial species, it could be possible to expand the repertoire of molecules we would be synthesized through this kind of processes.

Moreover, if coupled with the degradation of organic matter in the anodic compartment, these technologies would be able to break down pollution in wastewater while producing useful compounds with lower energy requirements in comparison with traditional wastewater treatment techniques, thereby representing an attractive alternative for industrial and municipal effluent treatment plants, once properly developed.

In addition to the degradation of organic matter and pollutants, anodic processes can be intentionally applied for the partial oxidation of, i.e., methane to methanol and ethane to ethanol or other oxidative processes. This kind of application can be defined as electro-fermentation and will most probably have a great importance in various sectors including: food&beverage, green synthesis, and biotechnological processes in general.

1.2.2 Terminology of Microbial Electrosynthesis Systems (MES)

If we want to analyze the potential impact of the applications in this field on the environment, we need to start by considering the terminology. In this regard, Shröder *et al.* in [66] give us a useful explanation: *"Based on definitions for chemical synthesis, we propose to define microbial electrosynthesis (ME)..."* as follows: ME is "*...the execution of microbial catalyzed electrochemical reactions to transform a substance into a desired product. Thereby, microbial electrosynthesis reactions comprise anodic (oxidative) and cathodic (reductive) processes...*".

1.2.3 Actual shortcomings, limitations, strength, and advantages of MES and MFC technologies

At the current state of the art, Microbial Fuel Cells and Microbial Electrolysis (or electrosynthesis) Systems in particular still suffer from a lack of a complete understanding of the physical (bio-electro)chemical and biochemical phenomena that govern the underlying processes. This is also the cause of performance issues when compared to electrochemical catalysts and therefore renders MES a yet immature and commercially unfavorable technology [59]. Although other technologies like desalination were not commercially available until 30 years after their discovery, according to Prévoteau et al. several critical points need to be solved for this technology to be usable in industrial contexts in the next 10-20 years:

- nonselective production at low concentrations,
- generally low production rates,
- large ohmic drop in cells,

- low energy conversion efficiency,
- and high investment cost.

1.2.4 The concept of microbial biotransformant, its advantages, and disadvantages over a traditional (electro)chemical catalyst

According to Harnisch and Shröder [22], a microbial cell performing biological transformation cannot be defined as a biocatalyst because it does not strictly adhere to the definition of catalyst: "*A catalyst, although being decisively involved in a reaction, is not consumed or altered by the reaction nor is it involved in the reaction's net-energy balance*" [46, 22], while microbial cells that are carrying out a biotransformation gain a certain amount of energy from the net reaction in order to multiply and perform other cellular activities [22].

The general definition of ME in 1.2.2 introduces the concept of biotransformant. A microbial biotransformant, in principle, has a few advantages over chemical catalysts [36]:

- self-regeneration capability ,
- self-assembly on the support (biofilm formation),
- no purification of the catalyst is needed,
- low cost,
- stability,
- robustness,
- and ample possibility of different output chemicals.

These advantages make microbial biotransformants good candidates for robust and cheap electrosynthesis of commodity and specialty chemicals, due to the high variety of microbial catalyzed reactions. This last trait, however, also constitutes the main challenge to the wide utilization of these microbial catalysts. In many

cases, the microbial strain responsible for the reaction is not well characterized, the mechanism that governs the reaction(s) is often not (well) understood, and many other problems exist. For example, the population dynamics of mixed cultures and the electron uptake mechanisms involved are not well studied [60] [62] .

If a model organism was to be utilized instead, most of these problems could be strongly alleviated if not completely eliminated. Moreover, most model organisms have already well-characterized genetic sequences and a fair number of them already have synthetic biology tools in a well-established state. These conditions enable new advantages if a model organism is employed as a microbial catalyst:

- possibility of modification of the output chemical(s) via genetic engineering,
- enhanced conversion efficiency,
- and higher selectivity toward the desired chemical.

1.3 An introduction to the electroactivity of microbes of relevant environmental interest

Shewanella oneidensis MR-1 is a gram-negative rod-shaped Gammaproteobacterium and a model microbe for the study of EET processes. Typical dimensions range between 2-3 μm in length and 0.4-0.7 μm in diameter. It is commonly found in marine and freshwater sediments and it is able to swim by the usage of a single polar flagellum [74].

Since 1988, the characterization of *Shewanellaceae* has allowed the discovery and classification of more than 40 species by the aid of 16S and DNA:DNA-hybridization techniques. Among the specimens characterized, the features that were revealed there were, for example, psychrotollerance, moderate halophilicity, and the ability of reducing and oxidizing an extremely wide variety of organic and inorganic compounds [25]. In addition, their ability to respire various metals and to produce hydrocarbons has sparked the interest on the characterization and biotechnological application of these bacteria.

Its ability of reducing metals has directed research toward bio-remediation applica-

tions, including those regarding nuclear wastes of industrial origin due to the fact that most of the metallic radionuclides include one or more redox states in which the oxides becomes insoluble [37].

Shewanella was identified in 1931 as one of the species of bacteria growing on putrid butter and first classified as part of the genus Achromobacter. Successively, its collocation was adjusted several times on the basis of its polar flagella, its status as a non-fermenting marine bacterium, and the guanine/cytosine content (% GC) of its DNA [25]. In 1985, 5S rRNA sequencing was used to support an entirely new name for the genus Shewanella [41].

1.3.1 The model microbe *Shewanella oneidensis* MR-1

A team of scientists discovered in 1980s inexplicably high levels of reduced manganese (Mn^{2+}) in New York's largest freshwater lake, Lake Oneida. Manganese generally exists in the environment in its oxidized form (Mn^{4+}) [50], and thus the researchers hypothesized that some biological process was reducing the manganese.

With experimental trials, they discovered a specie of Shewanella that respires by transferring electrons to Mn^{4+} [11]. In addition, oxidized manganese is not soluble, thus indicating that the bacteria had a way to transfer electrons to the metal outside of their cells to respire it.

Upon the rRNA sequencing, the isolate was characterized as a new Shewanella species, and named Shewanella oneidensis MR-1 ("manganese reducer") after the name of lake in which it was discovered. This strain was the first Shewanella genome to be sequenced, and thus it became a model system for the study of the genus [25].

1.3.2 Biofilm formation and electron transfer mechanism

The ability to respire insoluble compounds is a true biological feature that scientists have begun to deeply investigate. A key step to the successful continued reduction of extracellular metals is the formation of a biofilm by Shewanella on the already present metal oxide particles or other substrate. Biofilms facilitate close contact

between the bacteria and the oxidized metal.

A study by the group of Thormann et al. [71] investigated the mechanisms of biofilm formation in Shewanella oneidensis MR-1 on the surface of a glass slide in a flow cell. They reported that the microbes first attach and grow laterally until the majority of the surface available to them was covered by their cells. Then, Shewanella began to develop the biofilm vertically creating towering structures. Using mutagenesis experiments, the group discovered that the microbes do not need to swim to attach to the surface, although swimming is actually critical to the formation of three-dimensional structures. On the other hand, the biosynthesis of type IV pili is crucial for microbe-to-surface adhesion and the ability to retract them is required for lateral coverage of the biofilm.

The group also reported that Shewanella grow stronger biofilms, with greater microbe-to-surface interactions, when nutrient levels are poor, probably due to the fact that these bacteria can simply metabolize the nutrients aerobically rather than investing energy in the formation of biofilm for low energy-yielding respiration. However, typical anaerobic natural environments of Shewanella promote biofilm formation, and this in turn allow them to thrive on nutrients that most of other organisms cannot use.

Electron transfer players: Cytochromes and Riboflavin

Once the biofilm is formed, bacteria are obliged to transfer electrons from their cells to some electron acceptors to respire. Some of the most important parts of the pathway for electron transfer are called c-type cytochromes, which are heme cofactors containing polypeptides that associate small, reversible energy transitions with electron transfer. Cytochrome proteins consist of a protein structure including one or more heme groups.

Heme cofactor is composed of a ring of conjugated double bonds surrounding an iron atom. Double bonds and iron atoms can acquire and transfer electrons easily because they have narrowly spaced energy levels that facilitate small energy transitions.

There are various types of cytochromes in various kinds of microbial species, and *Shewanella oneidensis* MR-1 is known to include at least 42 putative cytochrome

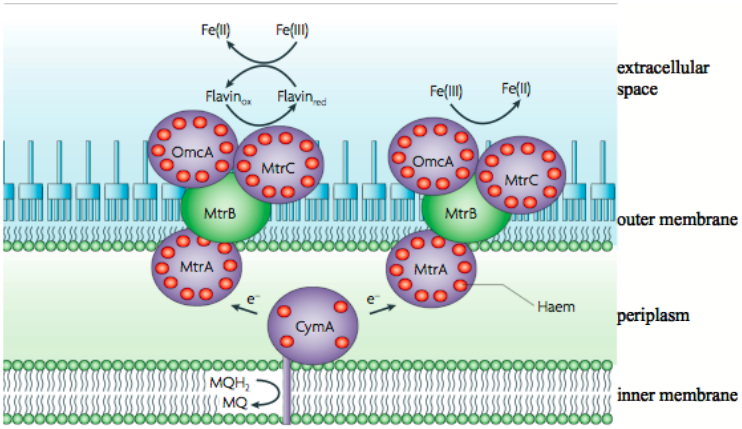

Figure 1.3. Cytochrome c molecules with multiple hemes transfer electrons from membrane soluble quinones in the inner membrane (MQH2), to the periplasm (CymA). Electrons then move through the outer membrane (MtrA, MtrB protein) to the extracellular surface (MtrC and OmcA), where they can contact insoluble metals directly (pathway to the right) or be shuttled by flavins to metals at a farther distance from the cell surface (pathway to the left)(Photo from Fredrickson, J., Romine, M., Beliaev, A. et al. Towards environmental systems biology of Shewanella. Nat Rev Microbiol 6, 592–603 (2008). https://doi.org/10.1038/nrmicro1947

c molecules in its genome [44]. The cytochrome c proteins of Shewanella involved in electron transport, have multiple heme groups and exist in the inner membrane (CymA), periplasm (MtrA), and the outer membrane (MtrC and OmcA). The outer membrane c-type cytochromes, MtrC and OmcA, are lipoproteins associated with the outer membrane protein MtrB (figure 1.3). They are fixed in the outer membrane by the Type II protein secretion pathway.

While being attached to the external side of the outer cell membrane, MtrC and OmcA cytochromes are exposed to the extracellular environment where they can get in contact with metals and other solid electron acceptors to which they transfer electrons. These outer membrane cytochromes are so crucial to metal reduction that *Shewanella oneidensis* MR-1 species that are missing OmcA and MtrC are 45% and 75% slower respectively at reducing MnO_2 than non-mutated strains [47]. While the functions of many of the other cytochrome c variants have to be discovered, some have been supposed to be involved in fumarate, nitrate, and dimethylsulfoxide (DMSO) reduction [19].

1.4 Purple Bacteria: Electron Acceptors and Donors

[from: Adessi, Alessandra, La Cava, Eugenio and De Philippis, Roberto. (2021) Purple Bacteria: Electron Acceptors and Donors. In: Jez Joseph (eds.) Encyclopedia of Biological Chemistry, 3rd Edition. vol. 2, pp. 305–314. Oxford: Elsevier.]

Purple bacteria form a heterogeneous group of microorganisms capable of growing under anoxic conditions by anoxygenic photosynthesis. They can be divided in purple non-sulfur bacteria, which are able to grow both phototrophically and in darkness, and purple sulfur bacteria, all of them capable to grow in the light but only few of them in the dark. The recent publication of several complete genome sequences of purple non-sulfur bacteria strains of the *Rhodopseudomonas palustris* and other species, pointed out the metabolic versatility of this group of bacteria.

Indeed, it was found that the genome of *Rps. palustris* contains all the genes needed for switching from chemotrophy to phototrophy, from organotrophy to lithotrophy, from heterotrophy to autotrophy. Under anoxic light conditions, *Rps. palustris* can use either the reducing power deriving from organic compounds, such as organic acids or aromatic compounds, or the electrons deriving from inorganic compounds, such as H_2, $S_2O_3^{2-}$ [28], NO_2^- [21], Fe^{2+} species and even electrodes of a microbial fuel cell [8, 7]. When growing chemotrophically in the presence of oxygen, respiration occurs and the reducing power can derive, as well as under anoxic light conditions, from either organic or inorganic compounds. When neither light nor oxygen is present, anaerobic respiration can take place, using NO_3^- or N_2O and NO as final electron acceptors [31, 33]. Moreover, purple sulfur bacteria are able to use sulfide as an electron donor, oxidizing it to elemental sulfur or even to sulfate, while only some non-sulfur bacteria can use S_2^-, but with different enzymatic pathways. Due to the remarkable complexity of the metabolism of purple bacteria, this work will mainly focus on the main electron acceptors and donors involved in the photosynthesis, in the respiration and in the extracellular electron transport.

1.4.1 The Electron Transport Chain (ETC)

The main stages of both photosynthesis and respiration processes occur in membranes. Therefore, membranes are the site of ATP generation for purple bacteria and in both processes, ATP is formed as a result of the proton motive force generated along with electron translocation through the ETC. These two processes, however, take place in different sites of the purple bacterial membrane: the cytoplasmic membrane (CM) harbors the components of the respiratory apparatus, while the photosynthetic apparatus is located in the so-called intracytoplasmic membranes (ICM) [30], which originate from the invagination of the CM and can take different forms throughout the purple bacteria group. Though aerobic respiration and anoxygenic photosynthesis would appear two distinct and very different processes, they have many common issues.

Anoxygenic Photosynthesis

The specificity of purple bacteria is their ability to form their energy carrier (ATP) in absence of oxygen by using sunlight as a source of energy. In this process, bacteriochlorophylls are both the primary electron donors and the final electron acceptors, as anoxygenic photosynthesis is a cycle (Fig. 1.4) [6].

A photon is absorbed by the light harvesting (LH) complexes that funnel the excitation towards bacteriochlorophylls in the reaction center (RC) where charge separation occurs [13]. This energy is used for the release of an electron which reduces the quinone Q. Once the quinone is doubly reduced (i.e. after a second photon is captured) it picks up protons from the cytoplasmic space and translocates through the membrane to reach the cytochrome bc1 complex.

Here electrons are addressed to the cytochrome c2 (Cyt-c2) while protons are released in the periplasmic space. Cyt-c2 is then able to reduce the oxidized primary electron donors in the RC, thus closing the cycle [6]. The protons accumulated in the periplasm form an electrochemical gradient which is used by the ATP-synthase to generate ATP.

The electron cycle is opened only by the "Δp-driven reversed electron transport" (indicated by the thin blue arrows in fig. 1.4), i.e. by the action of both the NADH

dehydrogenase working in the "reversed" way to reduce NAD^+ to NADH, and the succinate dehydrogenase also working "backwards" reducing fumarate to succinate. As those two enzymes are able to catalyze both the forward and reverse reactions, the force that drives the direction is the presence or absence of the products; in particular the reversed reactions are ways to get rid of the possible excess of the reduced quinol. The reversed NADH dehydrogenase reaction is also the way to refurnish the cell with NADH reducing equivalents.

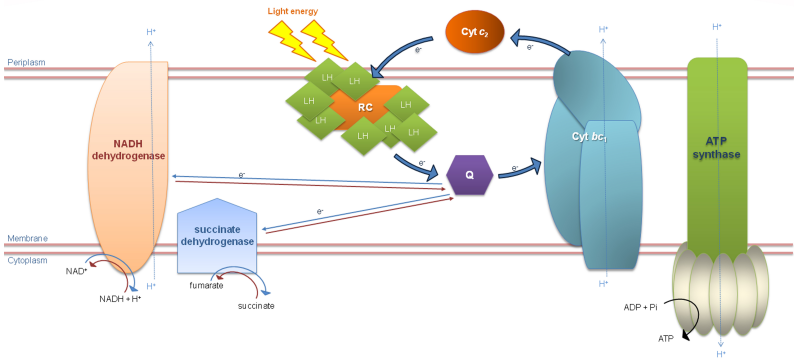

Figure 1.4. Anoxygenic photosynthesis cycle in *Rhodopseudomonas palustris*

Respiration

In the presence of O_2, anoxygenic photosynthesis in purple bacteria is inhibited and the ATP is synthesized through aerobic respiration (Fig. 1.5) [30]. The reducing power carried by NADH is transferred, by the action of NADH dehydrogenase, to a quinone. The quinone can also be reduced by the succinate dehydrogenase but, in this process, there is no proton translocation. The reduced quinone migrates through the membrane and can be oxidized both by the quinol oxidase, with oxygen as the electron acceptor, or by the bc1 complex, that functions (exactly as in photosynthesis) as a proton translocating step and transfers the electrons to the Cyt-c2. This soluble protein is, in respiration, oxidized by the Cyt-cbb3 oxidase which drives the reducing power to a molecule of O_2. As in photosynthesis, the protons accumulated in the periplasm form an electrochemical gradient which is used by the ATP-synthase to generate ATP.

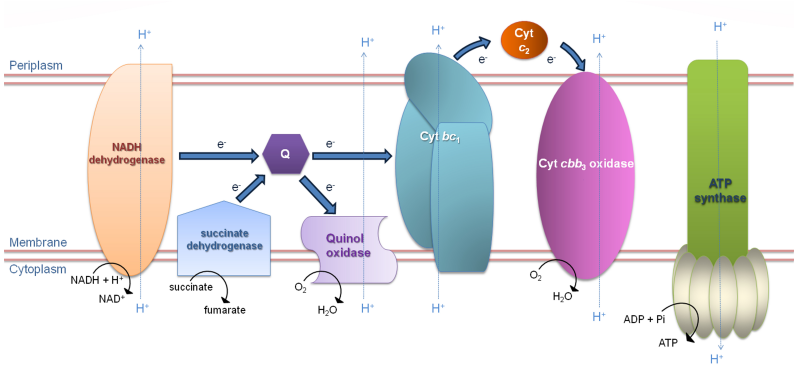

Figure 1.5. Respiration in *Rhodopseudomonas palustris*

1.4.2 The role of the quinone pool

As discussed above, purple bacteria have a very versatile metabolism. The regulation of the different metabolic behaviors is headed by the RegA/RegB system, which regulates photosynthesis, respiration, nitrogen and carbon fixation. This regulon gathers an integrated signal inclusive of environmental and cellular stimulations [30]. An important integrative signal coming from the cell is its redox state, which undergoes different values depending on the different metabolic conditions. This signal is mediated by the quinone pool, which holds a crucial role for the energetic processes in the cell, as it is schematically shown in figure 1.6.

1.4.3 Electron Acceptors and Donors Common in Photosynthesis and Respiration

The Ubiquinol:Cytochrome c Oxidoreductase (or Cytochrome bc1 Complex)

The ubiquinol:cytochrome c oxidoreductase is part, as previously shown, of both photosynthetic and respiratory ETC as its role is to oxidize the lipid soluble quinol and transfer its electrons to c-type cytochromes [15]. The overall reaction is the following equation (1.4.3.1), where QH_2 indicates the reduce quinol, while H_c^+ and H_p^+ indicate protons in the cytoplasmic and in the periplasmic space, respectively:

$$QH_2 + 2\,\text{Cyt–}c_2^{3+} + 2\,H_c^+ \rightarrow Q + 2\,\text{Cyt–}c_2^{2+} + 4\,H_p^+ \qquad (1.4.3.1)$$

As cytochromes are able to accept only one electron at a time, quinones have to

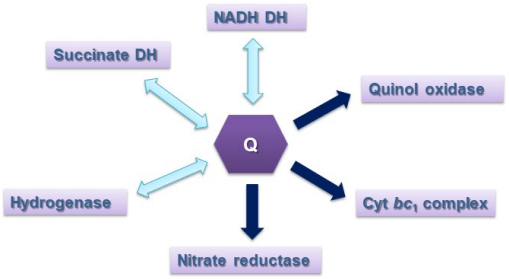

Figure 1.6. Functions of quinone in *Rhodopseudomonas palustris*. Light cyan double edged arrows mean bidirectional electron transfer while dark blue single edged arrows mean unidirectional electron transfer.

release their reducing equivalents one by one, and this shift from two-electrons to a one-electron process is managed by Cyt–bc_1 thanks to its architecture and cofactors [15].

This protein complex is a dimer and each monomer is composed of three subunits and contains four redox-active metal centers forming two distinct ETC: a low potential chain that transfers electron from the QP (P = membrane P face) site to the QN (N = membrane N face) site through two b-type hemes, namely Cyt–bL (L=low potential) and Cyt–bH (H=high potential), and a high potential chain, formed by a [2Fe-2S] cluster and a c-type heme covalently bound to the protein (Cyt–c_1), that makes electrons flow from the QP site to the oxidized Cyt–c_2 [9, 14, 15].

The quinol (QH_2) binds to the QP site where a bifurcation occurs. The electron that takes the low potential chain easily passes from the Cyt–bL to the Cyt–bH, as the first has a midpoint potential of about - 90 mV and the second of about + 50 mV. This high energetic step is necessary to compensate the otherwise unfavorable passage of a negative charge through the membrane from the P to the N face.

Close to the Cyt–bH site is located the QN site, where a quinone is reduced

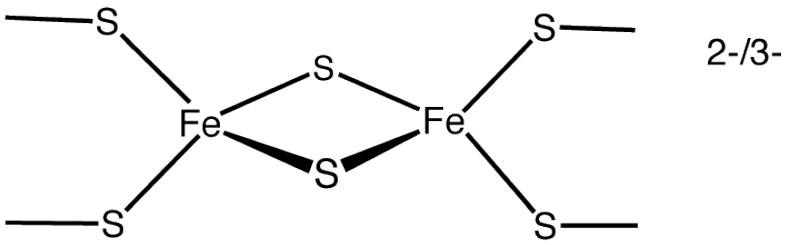

Figure 1.7. The Fisher's projection representation of a 2Fe-2S cluster

to semiquinone by the reduced Cyt–bH. This process, which is unfavorable due to this potential difference (from + 50 to –180 mV), occurs due to the protein-quinone interactions, which make the quinone potential more positive. The semiquinone is hold in the QN site until a second electron takes the low potential chain and reduces it to QH_2 [9]. The electron that takes the high potential chain reduces the [2Fe-2S] cluster, which, in this state, shows a higher affinity to the Cyt c1 that is almost 25 Å away.

This affinity makes the protein literally turn close to Cyt–c_1, so that the electron can reach the c1-heme. The oxidized [2Fe-2S] cluster is then more affine to the QP site and turns close to it. Midpoint potentials have been measured for the [2Fe-2S] cluster but the values depend dramatically on the occupant of the QP site; with the native Q bond, the midpoint potential is about + 320 mV; Cyt c1 has a midpoint potential of about + 230 mV. The reduced Cyt–c_1 is able to transfer its electron to the Cyt–c_2 that would close the photosynthetic cycle reducing the RC's P dimer.

1.4.4 Cytochromes

Cytochrome c2 is a single-heme soluble periplasm-located protein and acts as an electron deliverer. It accepts electrons from the Cyt–c_1 of the bc_1 complex and is present both in the photosynthetic process and in respiration: respectively, it reduces the P+ dimer to P, which is thus able to start a new photosynthetic turn, or reduces the cytochrome cbb_3 oxidase and in some organisms (*Rhodobacter sphaeroides*) also the cytochrome aa3 oxidase [16].

The underlying process for electron transfer at this step is Cyt–c_2 docking: many models have been proposed and many kinetic studies have been carried out to

determine the Cyt c2-RC interaction; it can be said that the docking is possible mainly due to electrostatic interactions, but also short-range interactions and H-bonds play a role as well.

After the protein docking, the most likely electron transfer pathway proceeds from the heme edge via Tyr L162 to the bacteriochlorophyll dimer, in a µs-scale process. The c2 heme midpoint potential varies between + 260 and + 360 mV, depending on purple bacteria strains [43].

The RC of *Blastochloris viridis* contains a non-dissociating tetraheme cytochrome molecule that facilitates the electrons flowing from Cyt c2. The electron transfer between the cytochrome and primary donor is about three times faster in *Blc. viridis* than in *Rba. sphaeroides*. This may be due to a different path-length (the distance between conjugated atoms on the heme and primary donor is 12.3 Å in *Blc. viridis* compared to 14.2 Å in *Rba. sphaeroides*) [3].

Cytochromes other than Cyt c2 are synthesized by purple bacteria in different metabolic phases: isocytochrome c2 and cytochrome cy (the latter membrane-bound) are present preferably in the presence of O2, while Cyt c2 transcription is increased in anoxic conditions, thus revealing that Cyt c2 is mainly involved in photosynthesis, while iCyt–c_2 and Cyt–cy are involved in respiratory pathways.

NADH-dehydrogenase

NADH dehydrogenase was defined as "The Most Complex Complex" by Tomoko Ohnishi in 1993 [52]. It is an L-shaped transmembrane complex, the largest of the bacterial electron transfer complexes as it is composed of 14 subunits; electron flow is mediated by a flavin mononucleotide (FMN) cofactor and 9 Fe/S centers, two [2Fe-2S] and seven [4Fe-4S] as described for *Thermus thermophilus*; one of the tetranuclear clusters is prokaryote-specific [5, 10].

This complex transfers electrons from NADH (- 320 mV) to ubiquinone (+ 90 mV). The primary electron acceptor is FMN (- 380 mV), then the electron passes through the linear pathway created by seven [Fe-S] clusters. The potentials of 6 of them vary between - 300 and - 230 mV; the other has a pH dependent midpoint potential ranging between - 20 and - 160 mV and is probably the last to be reduced

[10]. This enzyme mediates the overall reaction (1.4.4.1) (2) by which 4 cytoplasmic protons are released in the periplasmic space:

$$\mathrm{NADH} + 5\,\mathrm{H_c^+} + \mathrm{Q} \rightarrow \mathrm{NAD^+} + \mathrm{QH_2} + 4\,\mathrm{H_p^+}(2) \qquad (1.4.4.1)$$

This enzyme can also work in the reverse direction, in particular in phototrophic growth conditions in presence of a high QH2/Q ratio, to synthesize NADH reducing equivalents [10, 65].

Succinate dehydrogenase

The succinate dehydrogenase is a membrane-bound flavoprotein that is part of both the ETC and the TCA cycle; it transfers electrons from succinate to quinones, as indicated in reaction (3), and no proton translocation occurs [18].

$$\mathrm{Succinate} + \mathrm{Q} \rightarrow \mathrm{QH_2} + \mathrm{Fumarate}(3) \qquad (1.4.4.2)$$

This enzyme contains different cofactors that create a track for electrons; namely a FAD molecule, a [2Fe-2S] cluster, a [4Fe-4S] cluster, a [3Fe-3S] cluster and a heme b. Depending on the cell energetic needs, the enzyme can also catalyze the reverse reaction, as can happen during photosynthesis (see Fig. 1.4). Succinate, as a nutrient, also possibly involved in the regulation of LHC production and degradation [18].

1.4.5 Electron Acceptors and Donors Specific of Photosynthesis: Electron Transfer in the Reaction Center

The reaction center (RC) of purple bacteria is an integral membrane protein complex composed of L, M and H subunits.
The H subunit contributes to the complex stability and is involved in proton binding and transfer, while L and M compose the core of the RC and embed 9 cofactors, symmetrically disposed in an A and a B branch as shown in figure 1.8:

- 2 bacteriochlorophyll a molecules that form a dimer (P) connecting the two branches,

- 2 monomeric bacteriochlorophyll-a molecules (BA and BB),
- 2 bacteriopheophytin-a molecules (HA and HB),
- 2 ubiquinone molecules (QA and QB),
- and an iron ion.

Some authors suggest also the presence of a carotenoid molecule located next to the BB monomer. Bacteriochlorophylls and bacteriopheophytins can be substituted by some other molecules of the same class [13].

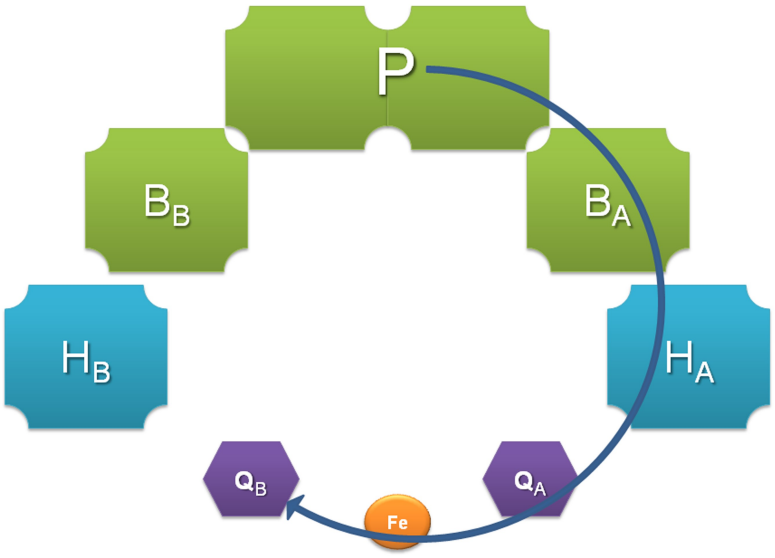

Figure 1.8. Schematic view of the reaction center of *Rhodopseudomonas palustris*

The midpoint potential of the cofactors is a critical point due to their own nature of electron transfer. The one directly measured is the midpoint potential of the P dimer, that is approximately + 500 mV for the P+/P couple. This positive potential makes it an optimal electron acceptor for Cyt–c_2. When a photon is conveyed to the P dimer an electron is raised to a higher energy level in a femtosecond time-scale; as Mg^{2+} is not able to release an electron, the electron comes from the tetrapyrrolic rings of the P dimer. The P^+/P^* couple has a very negative midpoint potential and is very unstable. The excited dimer P* transfers the electron, selectively through the A branch, to BA (in about 3.5 ps, in *Rba. sphaeroides*). Then, the electron is transferred to HA (in 0.9 ps, in *Rba. sphaeroides*); the overall transfer from P*

to HA takes from 3 to 5 ps, depending on bacterial species. The electron transfer from HA- to QA takes 200 ps, while the reduction of QB to QH2 takes place much more slowly, in about 100 µs. The oxidized P^+ is reduced back to P by an electron donated by Cyt–c_2: this transfer takes from 0.5 to 50 µs.

Purple bacteria export reducing equivalents in pair from the RC, and the molecule migrating from the RC to the other membrane proteins is the reduced quinol (QH2). Two electrons are needed to reduce the quinone to quinol, so, as the RC transfers electrons one by one, two quinones (QA and QB) are needed and act in a cycle in order to accumulate two reducing equivalents; after two RC turnovers a QH2 is released from the QB site [57].

QA and QB have different features: QA is very tightly bound in its site and can be under the quinone and the free-radical anionic semiquinone form ($QA^{\bullet-}$), while QB is reversibly bound and can be under the quinone, semiquinone and quinol form within the cycle. What makes the main difference between QA and QB (that in some species are chemically identical - for instance in *Rba. sphaeroides*) is the interaction with the protein in their binding sites. The $QA^{\bullet-}$/QA couple has a midpoint potential of about -180 mV. Then the $QA^{\bullet-}$ migrates to the QB site and here the second electron reduces it to Q^{2-}. The protons are captured from the cytoplasm during the acceptor quinone cycle, and will be released in the periplasm by the cytochrome bc1 complex to form the proton gradient needed for ATP synthesis [57]. The overall reaction can be resumed as follows (1.4.5.1):

$$2\,h\nu + Q + 2\,\text{Cyt–}c_2^{2+} + 2\,Hc^+ \rightarrow QH_2 + 2\,\text{Cyt–}c_2^{3+} \qquad (1.4.5.1)$$

QH2 is lipophilic enough to freely move throughout the membrane and transport its reducing power to different membrane-bound enzymes: in photosynthesis it can reach the cytochrome bc1 complex, but also NADH dehydrogenase and succinate dehydrogenase, thus opening the cyclic photosynthetic process with the "reversed electron flow". The "reverse" action of the NADH dehydrogenase is necessary to refurnish the cell of NADH.

1.4.6 Electron Acceptors and Donors Specific of Respiration

Evidences have shown that purple bacteria can contain different types of terminal oxidases: some species (e.g. *Rba. sphaeroides*) contain the cytochrome aa3 oxidase, the cytochrome cbb3 oxidase and a bb3-type quinol oxidase; some other species (e.g. *Rba. capsulatus*) contain only the cytochrome cbb3 oxidase and a bb3-type quinol oxidase.

In microorganisms that possess both cytochrome oxidases, the aa3-type is predominant when the cells are grown aerobically, while the cbb3-type is expressed mainly under microaerobic or photosynthetic conditions; otherwise the cbb3-type is the only cytochrome oxidase present [79].

All these proteins are part of the heme-copper oxidase (HCO) superfamily, but have significant differences in structure, in mechanisms and in the quantity and quality of cofactors. For example, aa3-type oxidases contain a binuclear copper cofactor named copper A (CuA), which is absent both in cbb3-type and in quinol oxidases. As Cyt aa3 oxidase is not always present in purple bacteria, in this section will not be discussed.

Cytochrome cbb3 oxidase

Member of the HCO superfamily, Cyt cbb3 oxidase is constituted by four subunits and contains many cofactors: 2 b-type hemes, 3 c-type hemes, and a copper B (Cu_B) [58]. Cyt cbb3 oxidase passes electrons from the Cyt c_2 to O_2 pumping protons in the periplasm following the reaction (1.4.6.1):

$$2\,\text{Cyt–c}_2^{2+} + 4\,\text{H}_\text{c}^{+} + ½\text{O}_2 \rightarrow\ 2\,\text{Cyt–c}_2^{3+} + 2\,\text{H}_\text{p}^{+} + \text{H}_2\text{O}(5) \qquad (1.4.6.1)$$

Cyt–cbb_3 oxidase is composed by a catalytic subunit containing the active site formed of a high-spin iron atom coordinated by a b3 heme and a Cu_B. Electrons are transferred to the active site by a second, low-spin, b-type heme. Electrons get to the catalytic subunit through a path created by rising potential c-type hemes: soluble Cyt–c_2 binds close to the first c-type heme and the electron flows through and reaches the active site. Potentials have been measured and in depth described for the 5 hemes of a Cyt–cbb_3 oxidase of *Pseudomonas stutzeri*; in Table 1.1 are

reported those values.

Redox center	Midpoint potentials (mV)
heme b	+310 ÷ +265
heme b3	+225
heme c	+245 ÷ +215
heme c	+245 ÷ +205
heme c	+185 ÷ +105

Table 1.1. Hemes of the Cyt–cbb$_3$ oxidase with their midpoint potentials –[Data refer to *Pseudomonas stutzeri* Cyt–cbb$_3$ oxidase]

As already mentioned, this enzyme can be present at low levels during photosynthesis that in purple bacteria takes place under anaerobic conditions. This evidence suggested another enzymatic function, i.e. the reduction of substrates other than oxygen.

Quinol oxidase

Quinol oxidase operates in order to equilibrate the QH_2/Q ratio, oxidizing quinols to quinones as indicated in the following reaction (1.4.6.2):

$$QH_2 + 2\,H_c^+ + ½O_2 \rightarrow\ Q + 2\,H_p^+ + H_2O \qquad (1.4.6.2)$$

The catalytic subunit is organized as in Cyt–cbb$_3$ oxidase and the reaction mechanism is the same, but the difference stands in the absence of the c-type hemes [69]. This enzyme pumps protons in the periplasmic space but less efficiently than the bc1- cbb3 system. For this reason this oxidase is mainly expressed under microaerophilic condition to avoid an over-reduction of the quinone pool. It was shown, in *Rba. capsulatus*, that Cyt–cbb$_3$ oxidase is a low O_2 affinity oxidase operating under conditions of high O_2 concentration, while quinol oxidase is a high O_2 affinity oxidase, operating under conditions of low O_2 concentration. In this way, it is possible that all the available oxygen is used as an electron acceptor before switching to lower-yielding acceptors such as nitrate, DMSO or arsenate in the

anaerobic respiration process [17].

Many purple photosynthetic bacteria are able to use electron acceptors other than oxygen: some conventional substrates such as sulfur and nitrogen compounds, and some "exotic" substrates like DMSO (dimethylsulfoxide), TMAO (trimethylamine-N-oxide) and even arsenate and halogenated aromatics. All the enzymes catalyzing these reactions contain complex cofactors, such as molybdopterine, [Fe-S] clusters, tetraheme cytochromes [79].

1.4.7 Other Electron Acceptors and Donors

Hydrogen

Hydrogen can be an electron donor for purple bacteria, oxidized by a membrane bound hydrogenase which functions as a ubiquinone oxidoreductase. The reaction (1.4.7.1) can take place in both directions, depending on the presence or absence of the substrates.

$$H_2 + Q \leftrightarrow QH_2 \tag{1.4.7.1}$$

However, H_2 can also be produced in purple bacteria by nitrogenase which functions primarily as nitrogen fixing enzyme (1.4.7.2), but also functions (in absence of molecular N2) using protons as electron acceptors (1.4.7.3) to dissipate the excess of reducing power in the cell.

$$N_2 + 8\,H^+ + 8\,e^- + 16\,ATP \rightarrow\ 2\,NH_3 + H_2 + 16\,ADP \tag{1.4.7.2}$$

$$8\,H^+ + 8\,e^- + 16\,ATP \rightarrow 4\,H_2 + 16\,ADP \tag{1.4.7.3}$$

For these reasons the hydrogenase and nitrogenase are often synthesized together and are regulated by complex and integrated signals [1].

Nitrogen compounds

Purple bacteria can use oxidized nitrogen compounds as electron acceptors, carrying out denitrification. Many are complete denitrifiers, while some are so called partial denitrifiers, because of the four enzymes required for the nitrate reduction to N_2 not

all are ubiquitous.

Generally speaking, purple bacteria contain most commonly the periplasmic nitrate reductase (Nap), the copper containing nitrite reductase (Cu-Nir), the cytochrome c oxidase NO reductase (cNor) and the nitrous oxidoreductase (Nos); a few contain the membrane bound nitrate reductase (Nar) and the heme containing Nir (cd1-Nir), but none contains the quinol oxidizing Nor (qNor). Table 1.2 summarizes the steps of denitrification as it occurs in purple bacteria [67].

Enzymes involved	Reactions	Midpoint potentials (mV)
Nar_a or Nap_b	$NO_3^- \rightarrow NO_2^-$	+ 420
$Cu{-}Nir_c$ or $cd_1{-}Nir_d$	$NO_2^- \rightarrow NO$	+ 370
$cNor_e$	$NO \rightarrow N_2O$	+ 1100
Nos_f	$N_2O \rightarrow N_2$	+ 1350

Table 1.2. Enzymes involved in denitrification with their respective reactions and the midpoint potentials of the redox couples [67](Shapleigh, 2009). Nar_a: membrane bound nitrate reductase, Nap_b: periplasmic nitrate reductase, $Cu{-}Nir_c$: copper containing nitrite reductase, $cd_1{-}Nir_d$ heme containing Nir, $cNor_e$ cytochrome c oxidase NO reductase, Nos_f nitrous oxidoreductase.

[omissis]

1.4.8 Extracellular Electron Transport

Extracellular Electron Transport (EET) is a process in which the cell exchanges electrons trough the cell membrane with external electron acceptor or donor that can be a naturally occurring chemical compound or an artificial electrode [38, 70].

Among purple bacteria, a handful of strains of the species *Rps. palustris* [8, 7, 75] *Rba. capsulatus* [24, 23] are able to perform EET in either one or both directions directly or by the use of mediators. For the records, also a mixed culture dominated by green sulfur bacteria [4] was described having this capability. These bacteria are therefore able to either reduce or oxidize an extracellular solid like some types of iron oxide minerals or an artificial electrode or soluble molecule, while some species are even capable of carrying out both processes in different conditions and moments

depending on the environmental circumstances. In the case of outgoing electron flow the electrode acts as an anode and its atoms accept electrons that come from the degradation of organic matter. Oppositely, when the flow of the electrons is inward to the cytoplasm the electron acceptors are the enzymes responsible for the generation of reducing power (i.e. NADH-Quinone Oxidoreductase, Ferredoxin reductase complexes) and the electron donor is the electrode or other electron donating molecules. Normally this ability is stimulated by illumination although a strain of *Rps. palustris* is able to uptake smaller currents even in dark condition [7].

Bose *et al.* [8, 7] also observed that the cellular apparatus used for the electron exchange process is the PioABC complex, which is normally responsible for the phototropic oxidation of iron. The Pio operon encodes for PioA, a decaheme periplasmic protein, PioB, a porin placed on the outer membrane and PioC, a protein provided with a high potential iron sulfur cluster [7].

Another important characteristic of some *Rps. palustris* strains is the production of conductive nanofilaments [76] called Type IV pili, similar to those of Geobacter spp. and other microbes. These cellular appendages are composed of monomers of pilin [76], a protein that in some electroactive microbes has, with evolution, acquired an aminoacidic sequence in which several aminoacids with aromatic residues are aligned regularly within the tertiary structure. The alignment of these aminoacids in the tertiary structure is such that there is a superposition of the π-orbitals of the aromatic ring residues that is sufficient to confer metallic-like conductivity in some cases [27, 68]. The stacked π-orbitals of the aromatic residues allow the transit through the pilin monomer and ultimately through the length of the pili of holes and electrons with similar efficiency [68].

[omissis]

1.4.9 Nomenclature and abbreviations

Cytochrome c2 ($Cytc_2$),
Cytoplasmic Membrane (CM),
Extracellular Electron Transport (EET),
Intra-Cytoplasmic Membranes (ICM),

Light Harvesting (LH),

Microbial Electrolytic Cell (MEC),

Microbial Fuel Cell (MFC),

Quinol (QH2),

Quinone (Q),

Reaction Center (RC),

Polyhydroxyalkanoates (PHAs).

References

[1] Alessandra Adessi and Roberto De Philippis. “Photosynthesis and hydrogen production in purple non sulfur bacteria: fundamental and applied aspects”. In: *Microbial bioenergy: hydrogen production*. Ed. by Davide Zannoni and Roberto De Philippis. Vol. 38. Advances in photosynthesis and respiration: including bioenergy and related processes. ISSN: 1572-0233. Dordrecht: Springer Netherlands, 2014, pp. 269–290. ISBN: 978-94-017-8553-2.

[2] Muktak Aklujkar et al. “The genome sequence of Geobacter metallireducens: features of metabolism, physiology and regulation common and dissimilar to Geobacter sulfurreducens.” In: *BMC Microbiology* 9 (May 2009), p. 109.

[3] Herbert L Axelrod et al. “X-ray structure determination of the cytochrome c2: reaction center electron transfer complex from Rhodobacter sphaeroides.” In: *Journal of Molecular Biology* 319.2 (May 2002), pp. 501–515.

[4] Jonathan P Badalamenti, César I Torres, and Rosa Krajmalnik-Brown. “Light-responsive current generation by phototrophically enriched anode biofilms dominated by green sulfur bacteria.” In: *Biotechnology and Bioengineering* 110.4 (Apr. 2013), pp. 1020–1027.

[5] John M Berrisford, Rozbeh Baradaran, and Leonid A Sazanov. “Structure of bacterial respiratory complex I.” In: *Biochimica et Biophysica Acta* 1857.7 (July 2016), pp. 892–901.

[6] R E Blankenship. “Origin and early evolution of photosynthesis.” In: *Photosynthesis Research* 33.2 (Aug. 1992), pp. 91–111.

[7] A Bose et al. “Electron uptake by iron-oxidizing phototrophic bacteria.” In: *Nature Communications* 5 (Feb. 2014), p. 3391.

[8] Arpita Bose and Dianne K Newman. “Regulation of the phototrophic iron oxidation (pio) genes in Rhodopseudomonas palustris TIE-1 is mediated by the global regulator, FixK.” In: *Molecular Microbiology* 79.1 (Jan. 2011), pp. 63–75.

[9] Ulrich Brandt. “Energy conservation by bifurcated electron-transfer in the cytochrome-bc1 complex”. In: *Biochimica et Biophysica Acta (BBA) - Bioenergetics* 1275.1 (July 1996), pp. 41–46. ISSN: 0005-2728.

[10] Ulrich Brandt. “Energy converting NADH:quinone oxidoreductase (complex I).” In: *Annual Review of Biochemistry* 75 (2006), pp. 69–92.

[11] Susan D. Chapnick, Willard S. Moore, and Kenneth H. Nealson. “Microbially mediated manganese oxidation in a freshwater lake1”. In: *Limnology and Oceanography* 27 (Nov. 1982). ADS Bibcode: 1982LimOc..27.1004C, pp. 1004–1014.

[12] Susan E. Childers, Stacy Ciufo, and Derek R. Lovley. “Geobacter metallireducens accesses insoluble Fe(iii) oxide by chemotaxis”. en. In: *Nature* 416.6882 (Apr. 2002), pp. 767–769. ISSN: 1476-4687.

[13] Richard J. Codgell et al. “How purple photosynthetic bacteria harvest solar energy”. In: *Comptes Rendus Chimie* 9.2 (Feb. 2006), pp. 201–206. ISSN: 1631-0748.

[14] A R Crofts and E A Berry. “Structure and function of the cytochrome bc1 complex of mitochondria and photosynthetic bacteria.” In: *Current Opinion in Structural Biology* 8.4 (Aug. 1998), pp. 501–509.

[15] Antony R Crofts. “The cytochrome bc1 complex: function in the context of structure.” In: *Annual Review of Physiology* 66 (2004), pp. 689–733.

[16] F Daldal et al. “Mobile cytochrome c2 and membrane-anchored cytochrome cy are both efficient electron donors to the cbb3- and aa3-type cytochrome c oxidases during respiratory growth of Rhodobacter sphaeroides.” In: *Journal of Bacteriology* 183.6 (Mar. 2001), pp. 2013–2024.

[17] Sylvie Elsen et al. “RegB/RegA, a highly conserved redox-responding global two-component regulatory system.” In: *Microbiology and Molecular Biology Reviews* 68.2 (June 2004), pp. 263–279.

[18] Kathryn R Fixen, Yasuhiro Oda, and Caroline S Harwood. “Redox Regulation of a Light-Harvesting Antenna Complex in an Anoxygenic Phototroph.” In: *mBio* 10.6 (Nov. 2019).

[19] James K. Fredrickson et al. “Towards environmental systems biology of Shewanella”. en. In: *Nature Reviews Microbiology* 6.8 (Aug. 2008), pp. 592–603. ISSN: 1740-1534.

[20] Sylvia Gildemyn et al. “Integrated Production, Extraction, and Concentration of Acetic Acid from CO2 through Microbial Electrosynthesis”. In: *Environmental Science & Technology Letters* 2.11 (Nov. 10, 2015), pp. 325–328.

[21] Benjamin M Griffin, Joachim Schott, and Bernhard Schink. “Nitrite, an electron donor for anoxygenic photosynthesis.” In: *Science* 316.5833 (June 2007), p. 1870. ISSN: 1095-9203.

[22] Falk Harnisch and Uwe Shröder. “From MFC to MXC : chemical and biological cathodes and their potential for microbial bioelectrochemical systems”. In: *Chemical Society Reviews* 39.11 (2010), pp. 4433–4448.

[23] Kamrul Hasan et al. “Electrochemical Communication Between Electrodes and Rhodobacter capsulatus Grown in Different Metabolic Modes”. In: *Electroanalysis* 27.1 (Jan. 2015), pp. 118–127. ISSN: 1040-0397.

[24] Kamrul Hasan et al. “Electrochemical communication between heterotrophically grown Rhodobacter capsulatus with electrodes mediated by an osmium redox polymer.” In: *Bioelectrochemistry* 93 (Oct. 2013), pp. 30–36.

[25] Heidi H. Hau and Jeffrey A. Gralnick. “Ecology and Biotechnology of the Genus Shewanella”. In: *Annual Review of Microbiology* 61.1 (Oct. 2007), pp. 237–258. ISSN: 0066-4227.

[26] John F Heidelberg et al. “Genome sequence of the dissimilatory metal ion-reducing bacterium Shewanella oneidensis.” In: *Nature Biotechnology* 20.11 (Nov. 2002), pp. 1118–1123.

[27] Dawn E Holmes et al. “The electrically conductive pili of Geobacter species are a recently evolved feature for extracellular electron transfer.” In: *Microbial genomics* 2.8 (Aug. 2016), e000072.

[28] Jean J Huang et al. “Production of hydrogen gas from light and the inorganic electron donor thiosulfate by Rhodopseudomonas palustris.” In: *Applied and Environmental Microbiology* 76.23 (Dec. 2010), pp. 7717–7722.

[29] Ludovic Jourdin et al. “High Acetic Acid Production Rate Obtained by Microbial Electrosynthesis from Carbon Dioxide.” In: *Environmental Science & Technology* 49.22 (Nov. 2015), pp. 13566–13574.

[30] Steffen Klamt et al. “Modeling the electron transport chain of purple non-sulfur bacteria.” In: *Molecular Systems Biology* 4 (Jan. 2008), p. 156. ISSN: 1744-4292.

[31] J Klemme. “Dissimilatory nitrate reduction by strains of the facultative phototrophic bacterium Rhodopseudomonas palustris”. In: *FEMS Microbiology Letters* 9.2 (Oct. 1980), pp. 137–140. ISSN: 0378-1097.

[32] Sanela Lampa-Pastirk et al. “Thermally activated charge transport in microbial protein nanowires”. In: *scientificreports* 6 (2016). ISSN: 2045-2322.

[33] Frank W Larimer et al. “Complete genome sequence of the metabolically versatile photosynthetic bacterium Rhodopseudomonas palustris.” In: *Nature Biotechnology* 22.1 (Jan. 2004), pp. 55–61.

[34] Tapio Lehtinen et al. “Production of alkanes from CO2 by engineered bacteria”. In: *Biotechnology for Biofuels* 11.1 (Aug. 2018), p. 228. ISSN: 1754-6834.

[35] Kar Man Leung et al. “Shewanella oneidensis MR-1 bacterial nanowires exhibit p-type, tunable electronic behavior.” In: *Nano Letters* 13.6 (June 2013), pp. 2407–2411.

[36] Xian-Wei Liu, Wen-Wei Li, and Han-Qing Yu. “Cathodic catalysts in bioelectrochemical systems for energy recovery from wastewater.” In: *Chemical Society Reviews* 43.22 (Nov. 2014), pp. 7718–7745.

[37] Jonathan R Lloyd and Joanna C Renshaw. “Bioremediation of radioactive waste: radionuclide–microbe interactions in laboratory and field-scale studies”. en. In: *Current Opinion in Biotechnology*. Environmental biotechnology/Systems biology 16.3 (June 2005), pp. 254–260. ISSN: 0958-1669.

[38] Derek R Lovley. “The microbe electric: conversion of organic matter to electricity.” In: *Current Opinion in Biotechnology* 19.6 (Dec. 2008), pp. 564–571.

[39] Derek R. Lovley et al. “Geobacter metallireducens gen. nov. sp. nov., a microorganism capable of coupling the complete oxidation of organic compounds to the reduction of iron and other metals”. In: *Archives of microbiology* 159.4 (1993), pp. 336–344.

[40] Bradley G Lusk. “Thermophiles; or, the modern prometheus: the importance of extreme microorganisms for understanding and applying extracellular electron transfer.” In: *Frontiers in microbiology* 10 (Apr. 2019), p. 818.

[41] M. T. MacDonell and R. R. Colwell. “Phylogeny of the Vibrionaceae, and Recommendation for Two New Genera, Listonella and Shewanella”. en. In: *Systematic and Applied Microbiology* 6.2 (Sept. 1985), pp. 171–182. ISSN: 0723-2020.

[42] Florian Mayer et al. “Performance of different methanogenic species for the microbial electrosynthesis of methane from carbon dioxide.” In: *Bioresource Technology* 289 (Oct. 2019), p. 121706.

[43] L. Menin et al. “Role of HiPIP as electron donor to the RC-bound cytochrome in photosynthetic purple bacteria”. In: *Photosynthesis Research* (1998).

[44] Terry E. Meyer et al. “Identification of 42 Possible Cytochrome C Genes in the Shewanella oneidensis Genome and Characterization of Six Soluble Cytochromes”. In: *OMICS: A Journal of Integrative Biology* 8.1 (Jan. 2004), pp. 57–77.

[45] Kyle Michelson et al. “Nanowires of Geobacter sulfurreducens Require Redox Cofactors to Reduce Metals in Pore Spaces Too Small for Cell Passage”. In: *Environmental Science & Technology* 51.20 (Oct. 17, 2017), pp. 11660–11668. ISSN: 0013-936X.

[46] Alwin Mittasch. “Über Begriff und Wesen der Katalyse”. In: *Allgemeines und Gaskatalyse*. Springer, Vienna, pp. 1–51.

[47] Judith M. Myers and Charles R. Myers. “Role for Outer Membrane Cytochromes OmcA and OmcB of Shewanella putrefaciens MR-1 in Reduction of Manganese Dioxide”. In: *Applied and Environmental Microbiology* 67.1 (Jan. 2001), pp. 260–269. ISSN: 0099-2240.

[48] Mohamed Y El-Naggar et al. “Electrical transport along bacterial nanowires from Shewanella oneidensis MR-1.” In: *Proceedings of the National Academy of Sciences of the United States of America* 107.42 (Oct. 2010), pp. 18127–18131. ISSN: 0027-8424, 1091-6490.

[49] K H Nealson and D Saffarini. “Iron and manganese in anaerobic respiration: environmental significance, physiology, and regulation.” In: *Annual Review of Microbiology* 48 (1994), pp. 311–343.

[50] Kenneth H. Nealson, Andrea Belz, and Brent McKee. “Breathing metals as a way of life: geobiology in action”. en. In: *Antonie van Leeuwenhoek* 81.1 (Dec. 2002), pp. 215–222. ISSN: 1572-9699.

[51] Kelly P Nevin et al. “Microbial electrosynthesis: feeding microbes electricity to convert carbon dioxide and water to multicarbon extracellular organic compounds.” In: *mBio* 1.2 (May 2010), e00103–10–e00103–10. ISSN: 2150-7511.

[52] T Ohnishi. “NADH-quinone oxidoreductase, the most complex complex.” In: *Journal of Bioenergetics and Biomembranes* 25.4 (Aug. 1993), pp. 325–329.

[53] Akihiro Okamoto, Yoshihide Tokunou, and Junki Saito. “Cation-limited kinetic model for microbial extracellular electron transport via an outer membrane cytochrome C complex.” In: *Biophysics and physicobiology* 13 (May 2016), pp. 71–76.

[54] Akihiro Okamoto et al. “Bound Flavin Model Suggests Similar Electron-Transfer Mechanisms inShewanella andGeobacter”. In: *ChemElectroChem* 1.11 (Nov. 2014), pp. 1808–1812. ISSN: 2196-0216.

[55] Akihiro Okamoto et al. “Rate enhancement of bacterial extracellular electron transport involves bound flavin semiquinones”. In: *Proceedings of the National Academy of Sciences* 110.19 (May 7, 2013), pp. 7856–7861. ISSN: 0027-8424.

[56] Akihiro Okamoto et al. “Uptake of self-secreted flavins as bound cofactors for extracellular electron transfer in Geobacter species”. In: *Energy & Environmental Science* 7.4 (2014), pp. 1357–1361.

[57] M.Y Okamura et al. “Proton and electron transfer in bacterial reaction centers”. In: *Biochimica et Biophysica Acta (BBA) - Bioenergetics* 1458.1 (May 2000), pp. 148–163. ISSN: 0005-2728.

[58] Robert S Pitcher and Nicholas J Watmough. “The bacterial cytochrome cbb3 oxidases.” In: *Biochimica et Biophysica Acta* 1655.1 (Apr. 2004), pp. 388–399.

[59] Antonin Prévoteau et al. “Microbial electrosynthesis from CO2: forever a promise?” In: *Current Opinion in Biotechnology* 62 (Oct. 2019), pp. 48–57.

[60] Korneel Rabaey and René A Rozendal. “Microbial electrosynthesis - revisiting the electrical route for microbial production.” In: *Nature Reviews. Microbiology* 8.10 (Oct. 2010), pp. 706–716. ISSN: 1740-1526, 1740-1534.

[61] Tahina Onina Ranaivoarisoa et al. “Towards sustainable bioplastic production using the photoautotrophic bacterium Rhodopseudomonas palustris TIE-1”. en. In: *Journal of Industrial Microbiology & Biotechnology* 46.9 (Oct. 2019), pp. 1401–1417. ISSN: 1476-5535.

[62] Miriam A Rosenbaum and Ashley E Franks. “Microbial catalysis in bioelectrochemical technologies: status quo, challenges and perspectives.” In: *Applied Microbiology and Biotechnology* 98.2 (Jan. 2014), pp. 509–518.

[63] Xuyan Ru, Peng Zhang, and David N. Beratan. “Assessing Possible Mechanisms of Micrometer-Scale Electron Transfer in Heme-Free Geobacter sulfurreducens Pili”. In: *Journal of Physical Chemistry B* 123.24 (June 20, 2019), pp. 5035–5047. ISSN: 1520-6106.

[64] Scott H Saunders and Dianne K Newman. “Extracellular Electron Transfer Transcends Microbe-Mineral Interactions.” In: *Cell Host & Microbe* 24.5 (Nov. 2018), pp. 611–613. ISSN: 1931-3128.

[65] Patricia Saura and Ville R I Kaila. “Energetics and Dynamics of Proton-Coupled Electron Transfer in the NADH/FMN Site of Respiratory Complex I.” In: *Journal of the American Chemical Society* 141.14 (Apr. 2019), pp. 5710–5719.

[66] Uwe Schröder, Falk Harnisch, and Largus T. Angenent. "Microbial electrochemistry and technology: terminology and classification". In: *Energy & Environmental Science* 8.2 (2015), pp. 513–519. ISSN: 1754-5692.

[67] James P. Shapleigh. "Dissimilatory and assimilatory nitrate reduction in the purple photosynthetic bacteria". In: *The purple phototrophic bacteria*. Ed. by C. Neil Hunter et al. Vol. 28. Advances in photosynthesis and respiration. ISSN: 1572-0233. Dordrecht: Springer Netherlands, 2009, pp. 623–642. ISBN: 978-1-4020-8814-8.

[68] Chuanjun Shu et al. "Direct Extracellular Electron Transfer of the Geobacter sulfurreducens Pili Relevant to Interaromatic Distances." In: *BioMed research international* 2019 (Nov. 2019), p. 6151587.

[69] Danielle L Swem and Carl E Bauer. "Coordination of ubiquinol oxidase and cytochrome cbb(3) oxidase expression by multiple regulators in Rhodobacter capsulatus." In: *Journal of Bacteriology* 184.10 (May 2002), pp. 2815–2820.

[70] Kenya Tanaka et al. "Extracellular Electron Transfer via Outer Membrane Cytochromes in a Methanotrophic Bacterium Methylococcus capsulatus (Bath)." In: *Frontiers in microbiology* 9 (Nov. 2018), p. 2905.

[71] Kai M. Thormann et al. "Initial Phases of Biofilm Formation in Shewanella oneidensis MR-1". In: *Journal of Bacteriology* 186.23 (Dec. 2004), pp. 8096–8104.

[72] Yoshihide Tokunou, Kazuhito Hashimoto, and Akihiro Okamoto. "Acceleration of Extracellular Electron Transfer by Alternative Redox-Active Molecules to Riboflavin for Outer-Membrane Cytochromec ofShewanella oneidensis MR-1". In: *The Journal of Physical Chemistry C* 120.29 (July 2016), pp. 16168–16173. ISSN: 1932-7447.

[73] Yoshihide Tokunou, Kazuhito Hashimoto, and Akihiro Okamoto. "Extracellular Electron Transport Scarcely Accumulates Proton Motive Force in Shewanella oneidensis MR-1". In: *Bulletin of the Chemical Society of Japan* 88.5 (2015), pp. 690–692. ISSN: 0009-2673.

[74] Kasthuri Venkateswaran et al. “Polyphasic taxonomy of the genus Shewanella and description of Shewanella oneidensis sp. nov.” In: *International Journal of Systematic and Evolutionary Microbiology* 49.2 (1999), pp. 705–724. ISSN: 1466-5034,

[75] Krishnaveni Venkidusamy and Mallavarapu Megharaj. “A Novel Electrophototrophic Bacterium Rhodopseudomonas palustris Strain RP2, Exhibits Hydrocarbonoclastic Potential in Anaerobic Environments.” In: *Frontiers in microbiology* 7 (July 2016), p. 1071.

[76] Krishnaveni Venkidusamy et al. “Electron transport through electrically conductive nanofilaments in Rhodopseudomonas palustris strain RP2”. In: *RSC Adv.* 5.122 (2015), pp. 100790–100798. ISSN: 2046-2069.

[77] Heming Wang and Zhiyong Jason Ren. “A comprehensive review of microbial electrochemical systems as a platform technology.” In: *Biotechnology advances* 31.8 (Dec. 2013), pp. 1796–1807.

[78] Xue Wang et al. “Efficient Methane Electrosynthesis Enabled by Tuning Local CO2 Availability”. In: *Journal of the American Chemical Society* 142.7 (Feb. 2020), pp. 3525–3531. ISSN: 0002-7863.

[79] Davide Zannoni. “Aerobic and anaerobic electron transport chains in anoxygenic phototrophic bacteria”. In: *Anoxygenic Photosynthetic Bacteria*. Ed. by Robert E. Blankenship, Michael T. Madigan, and Carl E. Bauer. Dordrecht: Kluwer Academic Publishers, 1995, pp. 949–971. ISBN: 0-7923-3681-X.

Chapter 2

Results: Involvement of Proton Transfer for Carbon Dioxide Reduction Coupled with Extracellular Electron Uptake in *Shewanella oneidensis* MR-1

[published as: Eugenio La Cava, Alexis Guionet, Junki Saito, Akihiro Okamoto (2020), Electroanalysis, https://doi.org/10.1002/elan.201900686.]

2.1 Abstract

Microbial biosynthesis of hydrocarbon from CO_2 reduction driven by electron uptake process from the cathodic electrode has gained intensive attention in terms of potential industrial application. However, a lack of a model system for detailed studies on the mechanism of the CO_2 reduction hinders the improvement in efficiency for microbial electrosynthesis. Here, we examined the mechanism of microbial CO_2 reduction at the cathode by a well-described microbe for extracellular electron uptake, *Shewanella oneidensis* MR-1, capable of reducing gaseous CO_2 to produce

formic acid.

Using whole-cell electrochemical assay, we observed stable cathodic current production at -0.65 V vs Ag/AgCl KCl sat. associated with the introduction of CO_2. The observed cathodic current was enhanced by the addition of 4 µM riboflavin, which specifically accelerates the electron uptake process of MR-1 by the interaction to its outer-membrane c-type cytochromes. The significant impact of an uncoupler agent and a mutant strain of MR-1 lacking sole F-type ATPase suggested the importance of proton import to the cytoplasm for the cathodic CO_2 reduction. The present data suggest that MR-1 potentially serves as a model system for microbial electrosynthesis from CO_2.

2.2 Keywords

biosynthesis, electrosynthesis, whole-cell electrochemistry, proton, ATPase

2.3 Introduction and state of the art

Microbial electrosynthesis has a potential for industrial application in which electrons from cathode drive the metabolism of certain bacteria capable of electron uptake from extracellular solids [26, 14, 28]. Various systems have been reported for CO_2 reduction with multispecies consortia directed to hydrocarbon production [14, 20, 8, 25, 1]. However, the efficiency of such processes still requires a large improvement for practical use[27, 4]. Therefore, it is an important strategy to use model pure culture for understanding the mechanism of CO_2 reduction on the cathode.

To this end, a model system with the defined electron transport pathway and carbon metabolism is required for the detailed study on the mechanism of CO_2 reduction. In addition to bacterial strains e.g. *Sporomusa ovata* [20] and *Acidithiobacillus ferroxidans* [11, 33], a recent study reported that *Shewanella oneidensis* MR-1 is capable of CO_2 reduction with the electrode as a sole energy source [13]. *S. oneidensis* MR-1 is a model microbe for extracellular electron transport (EET) [23, 17, 19, 18, 2, 16, 9]. It possesses a full set of EET proteins, namely, c-type cytochromes (c-Cyts) that enable MR-1 cells to reduce and oxidize a variety of solid electron acceptors

and donors, respectively [9]. Moreover, because it is capable of secreting and using various flavin-like molecules that can bind, as cofactors, to the extracellular c-Cyts, the rate of EET is controllable in both anodic and cathodic reactions [15, 5, 21].

2.4 Aim of the study

It has been reported that MR-1 produced formic acid coupled with CO_2 reduction most likely by formate dehydrogenase associated with electron uptake from a copper cathode electrode [13]. However, whether the electron uptake coupled with CO_2 reduction is a direct process or mediated by hydrogen generated from the electrode was not clear. In this study, we investigated the mechanism of CO_2 reduction by whole-cell electrochemical assay with MR-1 on the electrode with scarce hydrogen evolution.

We electrochemically examined whether the direct electron uptake from the cathode, rather than indirect shuttling mechanism by hydrogen, could play an important role in CO_2 reduction. Also, because charge neutrality and proton localization were shown to be critical for EET kinetics [32, 24], we used proton carrier agents, CCCP ([(3-chlorophenyl)hydrazono]malononitrile), and a mutant strain lacking the gene encoding ATP synthase ΔATPase) to check the impact of proton localization on the current production coupled with CO_2 reduction.

2.5 Materials and methods

2.5.1 Bacteria pre-cultivation

S. oneidensis MR-1 was grown aerobically in 15 mL of Luria-Bertani (LB) medium (20 g L^{-1}, Becton Dickinson, Sparks, MD) at 303 K overnight in a shaken incubator as previously described [21]. The culture was then centrifuged at 6,000 g for 10 min, and the resultant cell pellet was re-suspended in 15 mL of defined medium (DM, [22]) supplemented with 10 mM lactate as the sole carbon source. This procedure was repeated twice but the last time the amount of medium was adjusted to obtain optical density at $\lambda = 600$ nm (OD600) of 0.5 in the final reactor. We used DM for Shewanella [22] with modification, containing double the amount of HEPES buffer,

10 mL of 100x trace minerals solution, 1 mL 1000X vitamin solution and all the other usual components, excluding: resazurin, yeast extract, ammonium chloride, and sodium hydrogen carbonate. The medium is amended with sodium hydroxide solution to pH 7.8. ΔATPase mutant was made as previously described, and kindly provided by Prof. Jeffery A. Gralnick at the University of Minnesota [10].

2.5.2 Three electrodes electrochemical cell

Electrochemical experiments were conducted under cathodic conditions after the formation of biofilm in a single chamber three electrodes system under anodic condition poised at +0.2 V vs Ag/AgCl KCl sat., as described in previous reports [21]. The three-electrode system consisted of an indium tin oxide (ITO) substrate (surface area of 3.1 cm^2) as the working electrode at the bottom of the chamber and Ag/AgCl electrode (KCl saturated) and a platinum wire, which were used as reference and counter electrodes, respectively. Five milliliters of DM containing lactate (10 mM) was deoxygenated by bubbling with N_2 and added to the electrochemical cell as an electrolyte. The reactor was maintained at a temperature of 303 K. A cell suspension of MR-1 in DM with OD_{600} of 0.5 was cultivated on the ITO electrode.

2.5.3 Overall methodology

To examine CO_2 reduction coupled with direct electron uptake by S. oneidensis MR-1, we first prepared the monolayer biofilm of MR-1 on the ITO electrode in a single-chamber three-electrode system as previously described [21]. Followed by electrochemical cultivation under the anodic condition at +0.2 V vs Ag/AgCl KCl sat. for 24h in the presence of lactate as sole electron donor, we subjected MR-1 biofilm to an electrode potential of -0.65 V after the replacement of electrolyte without lactate and any electron acceptors. A previous study demonstrated that current for hydrogen production on the ITO electrode at this electrode potential is at sub nano-amperes [7].

h

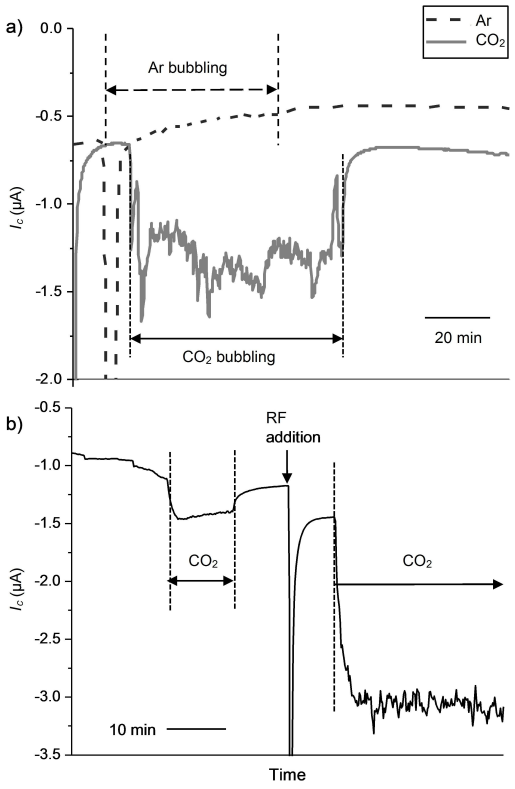

Figure 2.1. a)Time versus current production (I_c) by a monolayer biofilm of *S. oneidensis* MR-1 in an electrochemical system bubbled with Argon (dashed, black line) or CO_2 (full, gray line) poised at -0.65 V vs Ag/AgCl KCl sat. b) The effect of the addition of 4 μM riboflavin (RF) on I_c by MR-1 biofilm bubbled with CO_2 . For both panels, full- and dashed-line horizontal arrows indicate the time duration of gas bubbling.

2.6 Results

Upon CO_2 bubbling at the flow rate of 100 mL/min, a continuous cathodic current of approximately 0.2 - 0.3 µA cm^{-2} was observed, while no current increase was observed in the cell where Argon was bubbled Fig. (2.1a).

Stopping the flow of CO_2 resulted in an immediate current decrease to a level close to the original background current. This current change was reversible for more than five times with the small increase of the baseline, probably due to residual HCO_3^- or CO_2 in solution and/or inside the microbial cells.

The obvious cell number increase on the electrode surface was not observed

after the current production with CO_2 for 1 h compared with N_2 bubbling through microscopic observations on the electrode. The observed current production was approximately 30 times less than the cathodic current observed for oxygen reduction in MR-1 under air bubbling condition at 10 ml/min [29]. Because the contamination of oxygen in standard grade CO_2 gas (>99.995%) is less than 0.0005%, impurity oxygen would cause only two orders of magnitude lower current than the observed current production.

These results, therefore, strongly suggest that MR-1 biofilm use CO_2 as electron acceptor in the cathodic condition. Furthermore, given riboflavin enhances the rate of microbial electron uptake from cathode specifically via OM c-Cyts at a few micromolar concentration range [21], we examined the effect of riboflavin addition on the cathodic current production by MR-1 biofilm in the presence of CO_2. As we expected, the presence of 4 µM riboflavin significantly increased the cathodic current as shown in Fig 2.1b. These results strongly suggest that microbial electron uptake via OM c-Cyts drives CO_2 reduction.

Because*S. oneidensis* MR-1 has a metabolic pathway for CO_2 reduction that requires ATP consumption [23], we examined the role of ATP in the observed CO_2 reduction in MR-1 biofilm at -0.65 V by using mutant strain lacking sole F-type ATP synthase (F-ATPase) of MR-1 (ΔATPase). As expected, we observed significant suppression of the CO_2 reduction current compared with the wild-type (WT) strain of MR-1 (Fig.2.2a), suggesting the involvement of ATPase in the biological CO_2 reduction in MR-1. Meanwhile, F-ATPase operates not only on ATP production but also proton import to the cytoplasm. We therefore used proton carrier agents, CCCP ([(3-chlorophenyl)hydrazono]malononitrile) to examine if the recovery of proton uptake into the cytoplasm could enhance the rate of CO_2 reduction of ΔATPase. The addition of CCCP largely increased the current production of ΔATPase (Fig.2.2 b), while it did not cause a significant current increase in WT. This observation suggests that proton import to the cytoplasmic space limits the rate of CO_2 reduction in ΔATPase. Therefore, the large suppression of cathodic current in ΔATPase compared with WT is likely due to the difference in proton transport kinetics to the cytoplasmic space rather than ATP production. In addition, the

h

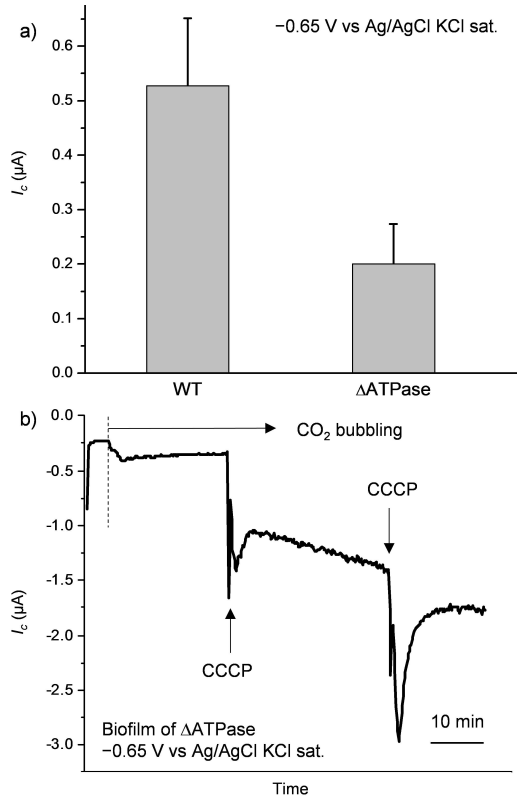

Figure 2.2. a) Average current of wild type and ΔATPase (n = 3 and n = 2 separated experiments, respectively) in cathodic conditions(potential of - 0.65 V vs. Ag/AgCl KCl sat. on the working electrode). b) The current profile of the ΔATPase deletion mutant of *S. oneidensis* MR-1 biofilm. Carbon dioxide was bubbled from the point indicated by the dashed line and CCCP was amended at the points indicated by vertical arrows (60 μM on the first and 120 μM on the second)

small current in ΔATPase suggests slower kinetics of proton transport in alternative routes, which may be represented by the Complex I working in reverse [3].

Although the pathway and product of the CO_2 reduction are not clear yet, the data for ΔATPase and CCCP addition support the idea that cathodic CO_2 reduction by MR-1 associated with proton import to the cytoplasm.

2.7 Discussion

It was proposed that CO_2 reduction to formic acid on an electrode surface poised at negative potential was catalyzed by the reverse reaction of formate dehydrogenase in the periplasm [12]. While this enzyme itself does not require proton transport across the inner membrane, the formate oxidation coupled with fumarate reduction generates proton motive force in *Shewanella oneidensis* MR-1 [12]. Therefore, its reverse reaction of CO_2 reduction coupled with extracellular electron uptake may be also associate with the proton import to the cytoplasm, in which electron input into menaquinone pool in the inner membrane was suggested to mediate proton transport. Thus, the proton-limited kinetics observed in this study may indicate that CO_2 reduction mainly happens in the periplasm of MR-1 as suggested in the previous work [13].

Alternatively, the idea of CO_2 reduction coupled with NADH consumption is consistent with our experimental results as well, because transmembrane proton transport from the periplasm to the cytoplasm is necessary to continuously reduce quinones and thus generate NADH in the cytoplasm. NADH generation may occur with the electrode with sufficiently negative potential [6], which might almost completely reduce quinone pool and drive the uphill reduction of NAD^+. Whereas the metabolic analysis has clarified that the tricarboxylic acid (TCA) cycle is complete under certain anaerobic conditions [31], some of key enzymes required for CO_2 reduction by reverse TCA cycle are absent in MR-1 [9].

Meanwhile, anaplerotic CO_2 assimilation is a possible pathway for CO_2 reduction coupled with NADH generation. Malate dehydrogenase can convert CO_2 into malate consuming NADH and pyruvate supplied from the preconditioning anodic condition [30]. The present work suggests that microbial cathodic CO_2 reduction in S. oneidensis MR-1 associates with direct electron uptake via OM c-Cyts and its kinetics is strongly influenced by proton transport. Because its electron transport chain and carbon metabolism are well described, MR-1 may have the potential to serve as a model system for electrosynthesis of hydrocarbon coupled with CO_2 reduction. Further investigation into other mutant strains allows deeper understanding of the enzymatic mechanism behind the CO_2 reduction associated with electron uptake.

2.8 Acknowledgement

This work was financially supported by a Grant-in-Aid for Research from the Japan Society for Promotion of Science KAKENHI (Grant Nos. 17H04969), and PRIME, the Japan Agency for Medical Research and Development (19gm6010002h0004).

References

[1] Suman Bajracharya et al. “Long-term operation of microbial electrosynthesis cell reducing CO2 to multi-carbon chemicals with a mixed culture avoiding methanogenesis.” In: *Bioelectrochemistry* 113 (Feb. 2017), pp. 26–34.

[2] Daniel Baron et al. “Electrochemical measurement of electron transfer kinetics by Shewanella oneidensis MR-1.” In: *The Journal of Biological Chemistry* 284.42 (Oct. 2009), pp. 28865–28873.

[3] John M Berrisford, Rozbeh Baradaran, and Leonid A Sazanov. “Structure of bacterial respiratory complex I.” In: *Biochimica et Biophysica Acta* 1857.7 (July 2016), pp. 892–901.

[4] Tatiana de Campos Rodrigues and Miriam A. Rosenbaum. “Microbial Electroreduction: Screening for New Cathodic Biocatalysts”. In: *ChemElectroChem* 1.11 (Nov. 2014), pp. 1916–1922. ISSN: 2196-0216.

[5] Harald von Canstein et al. “Secretion of flavins by Shewanella species and their role in extracellular electron transfer.” In: *Applied and Environmental Microbiology* 74.3 (Feb. 2008), pp. 615–623. ISSN: 1098-5336.

[6] Jiao Deng, Jesus A. Iñiguez, and Chong Liu. “Electrocatalytic Nitrogen Reduction at Low Temperature”. In: *Joule* (May 2018). Publisher: Elsevier.

[7] Xiao Deng et al. “Electron Extraction from an Extracellular Electrode by Desulfovibrio ferrophilus Strain IS5 Without Using Hydrogen as an Electron Carrier”. In: *Electrochemistry* 83.7 (2015), pp. 529–531. ISSN: 1344-3542.

[8] Jörg S Deutzmann and Alfred M Spormann. “Enhanced microbial electrosynthesis by using defined co-cultures.” In: *The ISME Journal* 11.3 (Nov. 2016), pp. 704–714.

[9] John F Heidelberg et al. “Genome sequence of the dissimilatory metal ion-reducing bacterium Shewanella oneidensis.” In: *Nature Biotechnology* 20.11 (Nov. 2002), pp. 1118–1123.

[10] Kristopher A Hunt et al. "Substrate-level phosphorylation is the primary source of energy conservation during anaerobic respiration of Shewanella oneidensis strain MR-1." In: *Journal of Bacteriology* 192.13 (July 2010), pp. 3345–3351. ISSN: 0021-9193.

[11] Shun'ichi Ishii et al. "A novel metatranscriptomic approach to identify gene expression dynamics during extracellular electron transfer." In: *Nature Communications* 4 (2013), p. 1601. ISSN: 2041-1723.

[12] Aunica L Kane et al. "Formate Metabolism in Shewanella oneidensis Generates Proton Motive Force and Prevents Growth without an Electron Acceptor." In: *Journal of Bacteriology* 198.8 (Apr. 2016), pp. 1337–1346.

[13] Quang Anh Tuan Le, Hee Gon Kim, and Yong Hwan Kim. "Electrochemical synthesis of formic acid from CO2 catalyzed by Shewanella oneidensis MR-1 whole-cell biocatalyst." In: *Enzyme and microbial technology* 116 (Sept. 2018), pp. 1–5.

[14] Christopher W Marshall et al. "Electrosynthesis of commodity chemicals by an autotrophic microbial community." In: *Applied and Environmental Microbiology* 78.23 (Dec. 2012), pp. 8412–8420. ISSN: 0099-2240.

[15] E Marsili et al. "Shewanella secretes flavins that mediate extracellular electron transfer." In: *Proceedings of the National Academy of Sciences of the United States of America* 105.10 (Mar. 2008), pp. 3968–3973. ISSN: 1091-6490.

[16] Leisa A. Meitl et al. "Electrochemical interaction of Shewanella oneidensis MR-1 and its outer membrane cytochromes OmcA and MtrC with hematite electrodes". In: *Geochimica et Cosmochimica Acta* 73.18 (Sept. 2009), pp. 5292–5307. ISSN: 0016-7037.

[17] Ryuhei Nakamura, Kazuyuki Ishii, and Kazuhito Hashimoto. "Electronic absorption spectra and redox properties of C type cytochromes in living microbes." In: *Angewandte Chemie* 48.9 (2009), pp. 1606–1608.

[18] Ryuhei Nakamura et al. "Self-constructed electrically conductive bacterial networks." In: *Angewandte Chemie* 48.3 (2009), pp. 508–511.

[19] K H Nealson and D Saffarini. "Iron and manganese in anaerobic respiration: environmental significance, physiology, and regulation." In: *Annual Review of Microbiology* 48 (1994), pp. 311–343.

[20] Kelly P Nevin et al. "Microbial electrosynthesis: feeding microbes electricity to convert carbon dioxide and water to multicarbon extracellular organic compounds." In: *mBio* 1.2 (May 2010), e00103–10–e00103–10. ISSN: 2150-7511.

[21] Akihiro Okamoto, Kazuhito Hashimoto, and Kenneth H Nealson. "Flavin redox bifurcation as a mechanism for controlling the direction of electron flow during extracellular electron transfer." In: *Angewandte Chemie* 53.41 (Oct. 2014), pp. 10988–10991. ISSN: 1433-7851.

[22] Akihiro Okamoto et al. "Cell-secreted flavins bound to membrane cytochromes dictate electron transfer reactions to surfaces with diverse charge and pH." In: *Scientific Reports* 4.1 (July 2014), p. 5628.

[23] Akihiro Okamoto et al. "In vivo electrochemistry of C-type cytochrome-mediated electron-transfer with chemical marking." In: *Chembiochem* 10.14 (Sept. 2009), pp. 2329–2332.

[24] Akihiro Okamoto et al. "Proton Transport in the Outer-Membrane Flavocytochrome Complex Limits the Rate of Extracellular Electron Transport." In: *Angewandte Chemie* 56.31 (July 2017), pp. 9082–9086.

[25] Sunil A Patil et al. "Selective Enrichment Establishes a Stable Performing Community for Microbial Electrosynthesis of Acetate from CO ." In: *Environmental Science & Technology* 49.14 (July 2015), pp. 8833–8843.

[26] Korneel Rabaey and René A Rozendal. "Microbial electrosynthesis - revisiting the electrical route for microbial production." In: *Nature Reviews. Microbiology* 8.10 (Oct. 2010), pp. 706–716. ISSN: 1740-1526, 1740-1534.

[27] Miriam Rosenbaum et al. "Cathodes as electron donors for microbial metabolism: which extracellular electron transfer mechanisms are involved?" In: *Bioresource Technology* 102.1 (Jan. 2011), pp. 324–333.

[28] Daniel E Ross et al. "Towards electrosynthesis in shewanella: energetics of reversing the mtr pathway for reductive metabolism." In: *Plos One* 6.2 (Feb. 2011). Ed. by Shuang-yong Xu, e16649. ISSN: 1932-6203.

[29] Annette R Rowe et al. "Tracking Electron Uptake from a Cathode into Shewanella Cells: Implications for Energy Acquisition from Solid-Substrate Electron Donors." In: *mBio* 9.1 (Feb. 2018).

[30] L Stols and M I Donnelly. "Production of succinic acid through overexpression of NAD(+)-dependent malic enzyme in an Escherichia coli mutant." In: *Applied and Environmental Microbiology* 63.7 (July 1997), pp. 2695–2701.

[31] Yinjie J Tang et al. "Anaerobic central metabolic pathways in Shewanella oneidensis MR-1 reinterpreted in the light of isotopic metabolite labeling." In: *Journal of Bacteriology* 189.3 (Feb. 2007), pp. 894–901.

[32] Yoshihide Tokunou, Kazuhito Hashimoto, and Akihiro Okamoto. "Extracellular Electron Transport Scarcely Accumulates Proton Motive Force in Shewanella oneidensis MR-1". In: *Bulletin of the Chemical Society of Japan* 88.5 (2015), pp. 690–692. ISSN: 0009-2673.

[33] Jorge Valdés et al. "Acidithiobacillus ferrooxidans metabolism: from genome sequence to industrial applications." In: *BMC Genomics* 9.1 (Dec. 2008), p. 597. ISSN: 1471-2164.

Chapter 3

Newly discovered electroactivity and N_2 fixing capability of *Rhodopseudomonas palustris* 42OL

3.1 Introduction

In PNSB, a few strains of the species *Rps. palustris* [6, 5, 24, 8] *Rba. capsulatus* [10, 9] are able to perform EET in either one or both directions directly or using mediators. When the flow of electrons is inward to the cytoplasm, the electron acceptors are the enzymes responsible for the generation of reducing power (i.e., NADH-Quinone Oxidoreductase, Ferredoxin reductase complexes) and the electron donor is the electrode or other electron donating molecule(s). In normal conditions, the EET process in PNSB is stimulated by illumination, although a strain of *Rps. palustris* is able to uptake smaller currents even without light irradiation [5].

Bose *et al.* [6, 5] also observed that the cellular apparatus used for the electron exchange process is the PioABC complex, which is normally responsible for the phototropic oxidation of iron. The Pio operon encodes for PioA, a decaheme periplasmic protein, PioB, a porin placed on the outer membrane and PioC, a

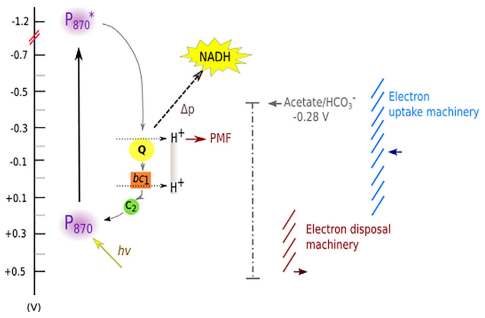

Figure 3.1. Energy diagram of *Rps. palustris* strain AZUL when in photo-heterotrophic growth mode, from "Electrochemistry of R. palustris Azul during phototrophic growth Electrochimica Acta, 2020, 355, 136757" [8]

protein provided with a high potential iron sulfur cluster [5]. In more recent times, a paper [8] from Guardia et al. hypothesized the presence of an alternative EET machinery due to the absence of the PioABC operon within the genome of *Rps. palustris* AZUL, a strain capable of both electron donation and uptake to and from electrodes.

Another important feature of some *Rps. palustris* strains is the production of conductive nanofilaments [25] called Type IV pili, similar to those of Geobacter spp. and other microbes. The alignment of these aminoacids in the tertiary structure is such that there is a superposition of the π-orbitals of the aromatic ring residues that is sufficient to confer metallic-like conductivity in some cases [11, 21]. The stacked π-orbitals of the aromatic residues allow the transit through the pilin monomer and ultimately through the length of the pili of holes and electrons with similar efficiency [21].

In addition, the presence of a triad of Nif operones, corresponding to the three types (Iron, Vanadium and Molybdenum) [18] of nitrogenase, makes this bacterium one of the most promising candidates for the electrochemically driven biological nitrogen fixation (e-BNF).

Rps. palustris 42OL used in this work was originally isolated from a pond containing waste waters of a sugar refinery [17], and although it was known to be a good hydrogen producer even in moderately high salinity [2] its electrochemical characteristics, if even present were not known at all. In this work, we planned to identify the

electrochemical characteristics and the ability of this strain to carry out e-BNF using nitrogen as the electron acceptor and the Working Electrode of an electrochemical cell as the electron donor.

3.2 Materials and methods

3.2.1 Stock culture and routine cultivation

Differently from what reported in the protocol from our lab [17, 1, 2], both the stock culture in agar and routine cultivation for electrochemical experiments were carried out in LB medium [3]. For stock culture tubes, renewals of the cultures were done every 5-6 months by pipetting 10 ml of melt LB-agar medium in 15 ml volume tubes. The medium was then allowed to solidify and successively inoculated by spiking with the pointy end of a sterile loop, previously immersed in fresh routine culture. The tubes were then sealed with parafilm tape.
For routine cultures, 45 ml liquid LB terrain was pipetted in 50 ml falcon tubes and inoculated either pipetting 200-1000 µl of previous liquid or with the pointy end of a sterile loop from the stock solid culture.
In either case, the cultures were left to grow for the following 15-20 days of daylight exposure (no artificial light source) in front of a southwest facing window at room temperature and without agitation, before they would be used. Periodically (once a week), routine culture tubes were gently turned upside down for a couple of times to avoid cell sedimentation and recirculate nutrients.
This culturing strategy allowed for longer stability and viability of routine and stock cultures compared with the RPN + carbon source medium.

3.2.2 Electrochemical cell and electrode preparation

Electrodes were cut in a rectangular or round shape from the stock material (carbon felt, Alfa Aesar, 99.0% carbon, 3.18 mm thick), with the rectangular being 6x17.5 cm (circa 0.5 cm less than the full internal circumference of the electrochemical cell) and the round ones being the same size of the bottom area of the cell.
Electrodes were used as they were without any further cleaning procedure, although

they were indeed sterilized in batches of singularly aluminium wrapped units to avoid contamination. Cleaning procedures were not necessary due to the high quality of the material and packaging in which it came from.

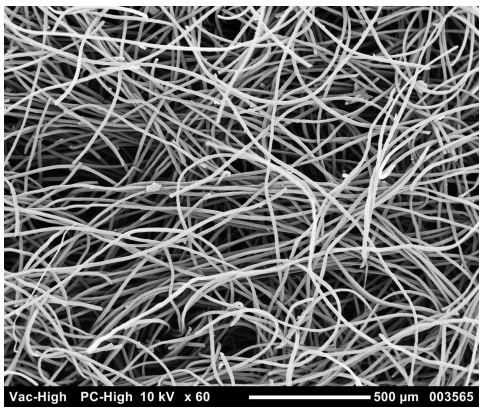

(a) 60X magnification of fresh electrode sample

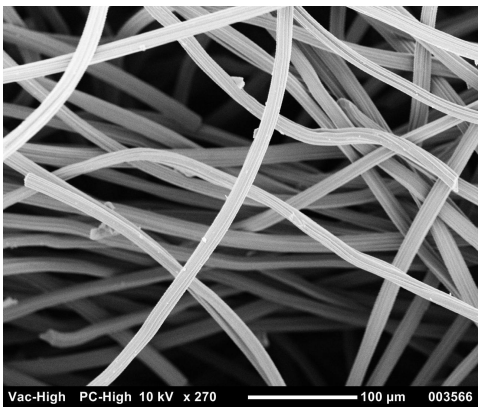

(b) 270X magnification of fresh electrode sample

Figure 3.2. Fresh non-colonized electrode at low and high magnification

Current collector and connection to the electrodes were made, respectively, with a copper wire and by mixing cyanoacrylate bicomponent glue with graphite powder (Pressol 1866121 10589, 034 Grafite, 50 gr, Amazon.it), at first. However, the connections were not stable in solution (noticeable corrosion was observed), and their contact resistances were not very reproducible and varied by one order of magnitude (130 Ω to 2000 Ω). Therefore, only the electrodes with a contact resistance below 150 Ω were utilized, while the others were rebuilt.

For the second set of experiments, we used titanium wire (Titanium Wire - Grade 1 - 0.25 mm ⌀ - 9.6 $\Omega\,m^{-1}$) passed through the electrode itself for connection and as the current collector. In this way, we hoped to avoid reproducibility issues and in fact, the resistance of the electrodes constructed in this way was oscillating between 35 and 45 Ω for circular ones (n=3) and 10 to 50 Ω for those of rectangular shape. The measurements were conducted using a multimeter set to continuity autorange mode and connecting one probe to the end of the connector wire and probing the farthest points of the electrode under test in various locations.

For the first series of experiments, we used hydrogen production *Rhodopseudomonas*

palustris medium (RPP) (≈3 mmol l^{-1} PBS) [4] as the washing and culture medium, with 3.6 g l^{-1} lactate as the carbon source.
For the following series, we decided to use a 100 mmol l^{-1} Potassium Phosphate Buffer (PPB) similarly to what is reported in [24] which we expected to respond well to our necessity of long-term operation of the electrochemical cell. The PPB was supplemented with 10ml/l of Wolfe's Trace Mineral Solution and 1.5 µg l^{-1} p-aminobenzoic acid [2] to promote cell metabolism and in the case of sole nitrogen gas bubbling, 3g/l of sodium acetate solution as carbon source.
The electrochemical cell used was a 012652 Water-Jacketed glass cell (100 ml) 50-80 ml sample vol (see fig.3.3). Reference and counter electrodes were respectively Ag−AgCl (3 mol l^{-1} KCl electrolyte) and platinum wire (Als-Japan). The reference electrode was kept in the dark in a 3 mol l^{-1} KCl solution to avoid drifting of the reference potential.
The cell was closed with its own Teflon cap, which is fitted with an oring gasket and ports for electrodes and gas purging. Purging was done with N_2 except for otherwise specified gas, at a flow rate of 5 ml min^{-1} to 10 ml min^{-1}, by a sterile needle immersed to the bottom of the cell.

A total of 50 ml of liquid volume was used for each experiment of the first series and the anodic part of second series, including:

- 37 ml bare RPP medium,
- 10 ml inoculum in RPP medium,
- 3 ml of concentrated acetate solution for a final concentration of 3 g l^{-1} acetate.

For the cathodic part of the second series of experiments, a total of 50 ml of liquid volume was used, including:

- 0.5 ml Wolfe's Trace Mineral solution,
- 0.5 ml p-Aminobenzoate solution to a final concentration of 1.5 µg l^{-1},
- 3 ml (or 0 ml when using 80:20 N_2:CO_2 purging gas), of concentrated acetate solution for a final concentration of 3 g l^{-1} acetate.

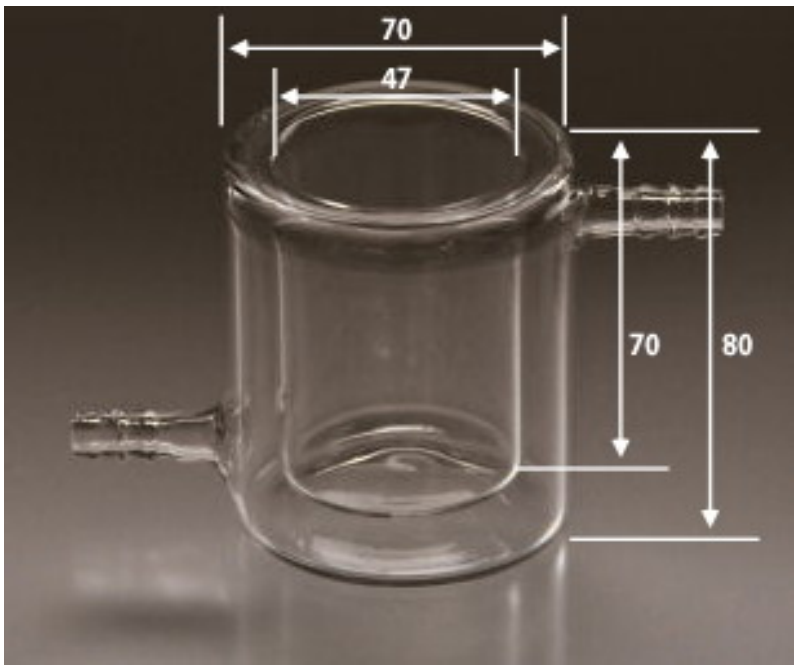

Figure 3.3. Dimensions in mm of the electrochemical cell used for the experiments

- 46 ml (or 49 ml when using 80:20 N_2:CO_2 purging gas), Potassium Phosphate Buffer at pH 7.2,

3.2.3 Measurements instrumentation

The potentiostat used for all measurements was an EmStat3+ from Palm Sense. The determination of the ammonia produced by the bacteria in cathodic condition was carried out by a colorimetric kit from Hannah Instruments and measured using the already calibrated spectrophotometric reader.

The preparation of the Working Electrode (WE) samples for SEM (on a Jeol Neoscope JCM-5000 Scanning Electron Microscope) micrography followed this protocol: immersion in Karnovsky fixative reagent [12] for 3 hours at 4°C, samples were then washed with cacolidate buffer 0.1 mol l^{-1} for 3 times and then transferred in Osmium tetroxide 1% solution for 2 hours, followed by a second cycle of three washes with cacolidate buffer and then submitted to dehydration cycle series of 30%, 50%, 70%, 90% and 100% ethanol with each dehydration step of 10 minutes repeated for 3 times. The dried samples were then metallized with gold in a SPUTTER-COATER

Jeol JFC-1300.

3.2.4 Estimation of bio-electrochemically produced ammonia

It is common knowledge that the electrochemically catalyzed production of any substance, solid, liquid, or gas follows the Faraday's Laws of electrolysis. Thus, if we want to estimate the production of our compound of interest, ammonia (NH_4^+), we can use Faraday's First Law of electrolysis that states: "in a given electrochemical reaction the mass (**m**) of substance that is deposited or released at the electrode surface is directly proportional to the amount of electricity or charge (**Q**) that passes through it." [7].

$$m = Z \cdot Q \tag{3.2.4.1}$$

where m is the mass in grams, Q is the charge in Coulombs, and Z is the proportionality number given in g/C. Proportionality constant that can be rewritten as the electrochemical equivalent (**E**), that is the mass produced or consumed at the electrodes by 1 Coulomb of charge, that would generate or consume 1 g equivalent of substance, divided by 1 F (or 96 485 C mol^{-1}). Now **Z** can be expressed as E/F, and if we rearrange equation 3.2.4.1 introducing Q = I, · t we get

$$m = \frac{E \cdot I \cdot t}{F} = \frac{M \cdot I \cdot t}{F \cdot z} \tag{3.2.4.2}$$

where **m** is the mass of the compound generated or consumed at the electrode (in grams), **M** is the molar mass of the of the specie (in g mol^{-1}), I is the current (in amperes), **t** is the time (in seconds), **F** is the Faraday constant or 96,485 **C**, and **z** is the number of electrons transferred per ion.

Thus in our case I is the sum of all 17280 averages of current over 5 seconds multiplied by the number of samples (5 per each set). The average of current over 5 seconds was chosen to obtain a number of samples (17280 or 86400/5 with 86400 being the number of seconds in 24h) to maintain a fine granularity of the current curves and evidence possible fluctuations due to reduction in N_2 flux with a number of data points conveniently low to work with.

3.3 Results

3.3.1 Electrode construction and reduction of electrical noise

From the very beginning, our strain showed good electrochemical activity, however in the chronoamperometry (CA) graphs, there are very evident current spikes that we could not explain by electromagnetic interference. After some research in the literature, we found a report [16], that evidentiate the photocatalitic activity of AgCl on the water splitting process according to the following reaction equation:

$$H_2O + 2\,Ag^+ \xrightarrow{h\nu,\mathrm{AgCl}} 2\,H^+ + \frac{1}{2}\,O_2 + 2\,Ag^0 \qquad (3.3.1.1)$$

Armed with this new knowledge, we designed a way to keep most of the light from reaching the reference electrode by wrapping it in denatured ethanol mopped Teflon tape. We tried to enhance the current production of the strain by the optimization of the construction of the cell's working electrode and cultivation medium.
At first, the electrode was connected to the potentiostat lead with a copper lead glued with a mix of cyanoacrylate-bicomponent glue and graphite powder, however this technique didn't give reproducible results. In fact, as stated in section 3.2.2, the resistance of the dried glue was varying by about 1 order of magnitude.
This prompted us to look for a different approach to the problem and our solution was to sew a titanium wire into the working electrode. This worked better than we expected and we were able to reduce the resistance of the electrode-current collector assembly to 10-50 Ω, less than a third of the best glue-graphite assembly (min value 130 Ω).
The resistance values obtained with the titanium current collector were comparable to those from my previous experiment with *Shewanella* I was using ITO coated glass as the electrode and a stainless steel crocodile connector, connected to a copper wire, as the current collector.

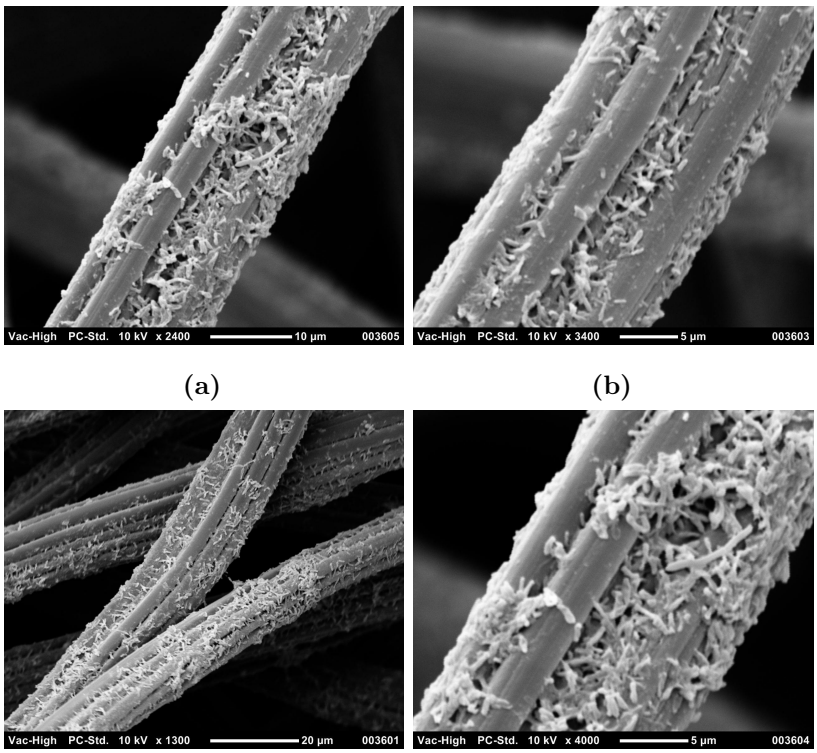

Figure 3.4. SEM pictures of a working electrode sample fixed with Karnovsky reagent and Osmium tetroxide after a few days of anodic cultivation. a: 2400X magnification, b: 3400X, c: 1300X d: 4000X.

3.3.2 Main results

Electrode colonization by *Rhodopseudomonas palustris* 42OL

From the SEM observation, we observed abundant cells adhering to the electrode fibers (see Figures 3.4 a,b,c,d) in the form of bundles and patches and this is in line with the findings on a report about another strain of the same specie [5].

This statement was confirmed by the following experiments and the SEM observations of the relative electrode specimens as can be noted from the Figure 3.4. It is quite obvious from those micrographs that the bacteria readily colonized the electrode and formed a biofilm on it. This direct observation reinforces and confirms the hypothesis that the current comes mainly from the attached microbes. It can also be noted that the bacteria grow in bundles as reported by other groups [5] and

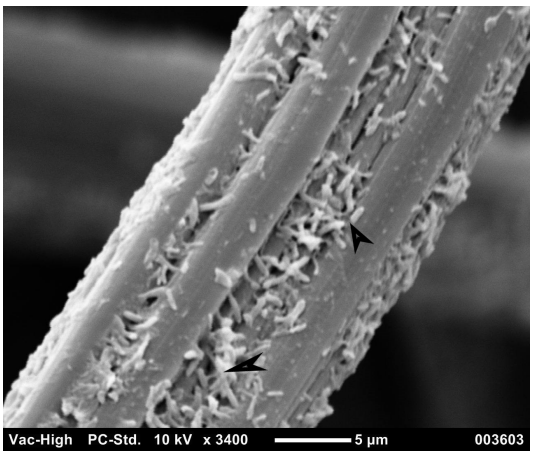

Figure 3.5. Pointed by the arrows there are filamentous structures that connect cell to cell and cell to electrode.

in some cases can produce long conductive appendages [25]. In our case we could not observe such long appendages, although as can be noted from Figure 3.5, we did observe some interconnected cellular appendages that seem to connect cells to other cells or to the electrode fibers. The structures we observed are quite different from those reported by Venkidusamy et al. in [25], in addition we cannot exclude the presence of the same structures in our sample simply because our SEM could not reach the same magnification as the one in [25].
Therefore, we believe that we are the first to observe the structures pointed by the arrows in Figure 3.5 in this specie.

Electroactivity of *Rhodopseudomonas palustris* 42OL

As appears from figure 3.6 it was clear from the very first experiments that the 42OL strain was indeed electroactive. The goodness of the measure was confirmed by the following experiment with sterile, non-inoculated medium, as can be seen in Figure 3.7 which shows negligible current in the said condition. This first set of trials was composed of three groups of experiments, Group 1 - 3 composed of 2, 3 and 9 chronoamperometric runs in anodic mode respectively, each run of 20 to 24 h duration.
All runs of groups 1-2 were conducted at +200 mV (vs Ag/AgCl$\cdot$ KCl_3M) thus circa

at +423 mV vs SHE, medium used was RPP supplemented with 3.6 g l^{-1} lactate. Group 1 is composed of chronoamperometric runs recorded on dates 17-18/11/20 and 18-19/11/20, while group 2 is composed of runs recorded on 23-24, 24-25, and 25-26/11/20. All recordings lasted between 20 and 24 hours.

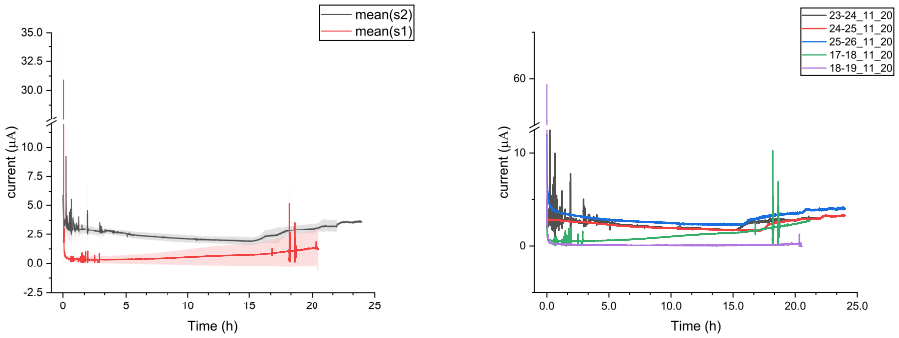

(a) **(b)**

Figure 3.6. (a) Mean of current measurements for run groups 1 (n=2) and 2 (n=3); the shaded area represents 1 SD at the sample position. (b) Single chronoamperometric runs for groups 1 and 2.

The first series of experiments in anodic mode showed that the strain was indeed electroactive, and that our setup required improvement in the part of connection with the electron collector of the electrode.

This suffered from high resistance and poor corrosion stability, especially in the cathodic part of the cyclic voltammetries, during which the epoxy resin degraded and swollen until when the electric contact was lost. This issue was solved using a titanium wire woven into the electrode fabric as the current collector in the second series of experiments.

In the first five runs, shown in fig 3.6 (b) and representing the first two sets of experiments there is a noticeable current although there are also noticeable spikes in the chronoamperometric measurements.

We noticed that pH of the medium in the cell was around 9 after several cycles of cyclic voltammetry (CV) the buffering capacity of bare RPP medium was not strong enough for counteracting the microbes metabolic activity under pure nitrogen stream.

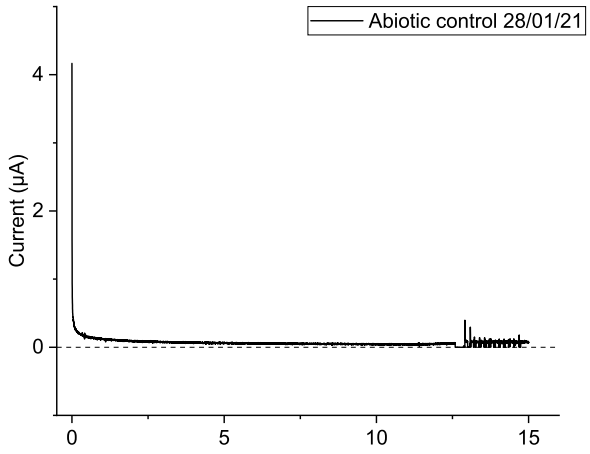

Figure 3.7. Abiotic control current measurement

This means that the current generated in the runs of the Experiment Group 1 of the preliminary trials comes from the microbes attached to the electrode. Figure 3.8 shows the effect of acetate on the production of current. In the previous groups, only the lactate included in the original formulation of the RPP medium was present as the carbon source, while in the runs of this group $3.0\,\mathrm{g\,l^{-1}}$ of acetate were added as an additional carbon source.

The rationale behind this choice is that acetate is a common substrate known to be utilized by other strains of the same species in various metabolic conditions and secondly, we found two papers [24, 25] regarding another electroactive *Rps. palustris* strain that successfully used that substrate in the electrochemical cultivation condition.

The effects were quite evident, with the current starting to grow almost exponentially after a 5h lag phase(lowest, black fitted curve), where presumably the cells had to adjust from the nutrient rich LB medium to the simpler carbon sources of the RPP + Acetate medium. An additional consideration is that the cells were harvested and inoculated in the electrochemical cell without any acclimation period in the new media to save time. In the following run (yellow curve in figure 3.8), the current was still growing and reached 30 µA from 10 of the previous run, while the cyan curve

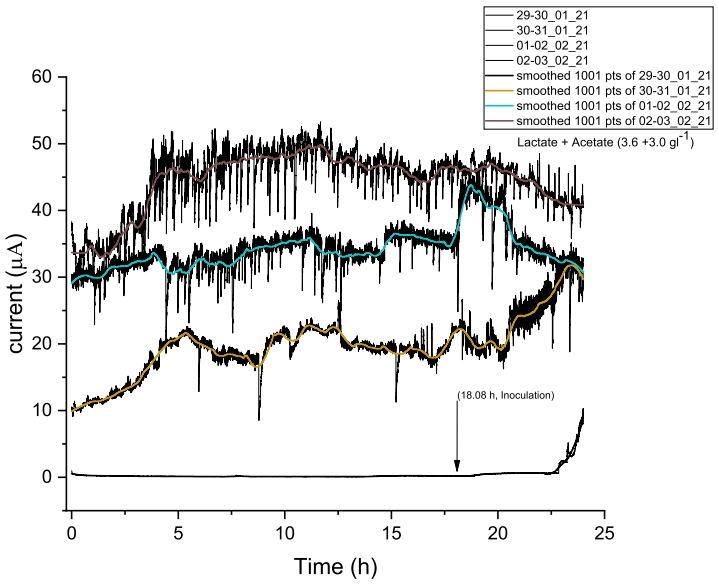

Figure 3.8. Group 3 of first series of experiments; same electrochemical conditions of groups 1 and 2 though the RPP medium was amended with $3.0\,\mathrm{g\,l^{-1}}$ Sodium Acetate.

peaked to ≈45 µA and brown reached 50 µA around the mid of the run.
As can be seen from the black tracks around the middle colorful average, the raw reads are still full of noise and spikes. This is due to the reference electrode being exposed to light and the fact that the first run is not affected is very likely due to the lack of current coming from the WE.

In the runs of figure 3.9 (from 5^{th} to 8^{th}) the current continued to grow and reached a peak of ≈ 130 µA then starting to decrease during the last (9^{th}) run. A possible explanation for the decreasing current in run 7^{th} and 9^{th} could be a combination of a few factors:

- the accumulation of metabolites in the medium,
- the limitation of nutrients and metabolites mass transfer from the media into the biofilm (and vice versa) as it grows thicker,
- and the exhaustion of nutrients in the medium.

All these three factors can contribute with different grades to the decrease of current, although they were not further investigated. Nonetheless, it should be

possible to design experiments to correlate the thickness and roughness of the biofilm (observing it by optical microscopy) and its mass transport characteristics while studying the metabolites and nutrients production/uptake, whereas a series of chromatographic analyses could monitor the concentrations of the chemical species of interests if a timely set of samples is taken from the cell during the experiments.

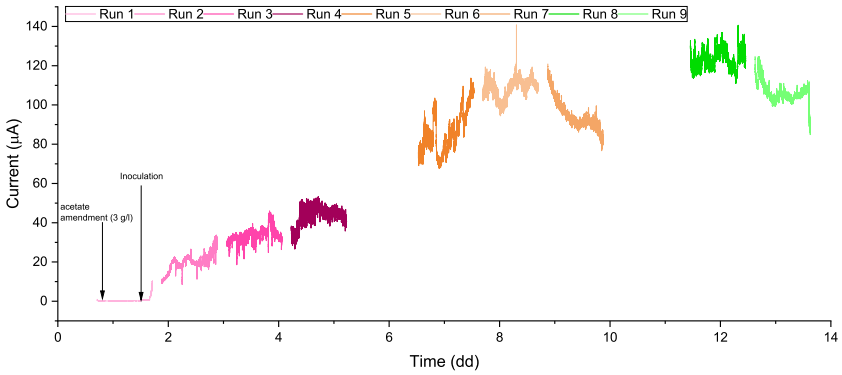

Figure 3.9. Complete group 3 of first series of experiments, chronoamperometric runs of 24h, with same electrochemical conditions of groups 1 and 2 (poised working electrode potential of $\approx 200\,\text{mV}$ vs SHE, N_2 purging of the cell at $10\,\text{ml}\,\text{min}^{-1}$) although the RPP medium was amended with $3.0\,\text{g}\,\text{l}^{-1}$ Sodium Acetate in addition to normally present Sodium Lactate. The intervals between the three sets of runs(1-4, 5-7, and 8-9) are due to cyclic voltammetry being performed. Differently from figure 3.8 all 9 runs of the serie are shown.

However, in our case this was beyond the scope of this research.

Preliminary results of electrochemically driven nitrogen fixation by *Rhodopseudomonas palustris* 42OL

For this experiment, few adjustments were made to the experimental design, namely the use of a minimal media (although amended with ammonium chloride) for the anodic precultivation, the use of a minimal media (without ammonia) for the cathodic part of the experiment and the use of a titanium wire to connect the electrode to the potentiostat. The last element has determined a significant reduction of spikes and

oscillation magnitude on the chronoamperometric tracks in both anodic and cathodic parts of the experiment, meaning that the new way of connecting the electrode to the potentiostat is more stable and less prone to produce electrical noise in the measurement.

The aim of this experiment was to determine if our strain was able to fix nitrogen in cathodic conditions. However, the analysis of the supernatant via colorimetric method did not show any relevant increase of ammonia in the media from the initial content that could result from the residual anodic medium impregnating the WE. It is possible that nitrogen was utilized by the bacteria in the biofilm, but with the current setup we could not determine whether this was true or not. Another aspect to consider is that the ammonium content is in equilibrium with gaseous ammonia, that in turn is carried away in the atmosphere by the constant stream of nitrogen bubbling in the cell since our cell is not a closed system.

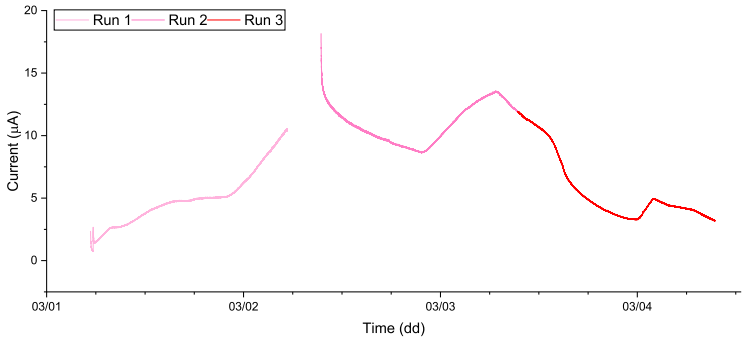

Figure 3.10. Three days precultivation of *Rps. palustris* strain 42OL before the N_2 fixing experiment. The rationale of the precultivation is to ensure proper time for attachment of the microbial cells to the WE. Run 1 - 3 represent the chronoamperometric measurement of current in the sole presence of acetate $3.0\,\mathrm{g\,l^{-1}}$ with reference electrode poised at 423 mV vs SHE.

As for what concerns the chronoamperometric runs, on one hand, a reduction in the current peak and current growth is evident in the anodic precultivation, even in comparison with the first three runs of the previous graph, and this is likely caused by a different ability of outputting the current due to lack of lactate in the medium.

The medium used in the previous set of experiments contains also this component at the concentration of 3.6 g/L, however, since we found that some literature reported acetate as a primary substrate for electrochemical experiments we decided to use conditions that were similar to those reported [22, 24].
Thus, for the cathodic part of the latter series of experiments we used a $100\,\mathrm{mmol\,l^{-1}}$ Potassium Phosphate Buffer (PPB) as specified in 3.2.2. The cathodic chronoamperometry shows a significant current uptake by the WE with a trend to a plateau from Run 1 to Run 7 and a recovery in Run 8 to Run 9 of figure 3.11. The current peaks at $\approx -9500\,\mu\mathrm{A}$ at the beginning of Run 1 is probably due to the electron starvation of cells in the biofilm after the polarization of the WE to $-650\,\mathrm{mV}$ vs Ag/AgCl RE ($\approx -425\,\mathrm{mV}$ vs SHE) and seem to indicate a metabolically active and healthy biofilm. We tend to exclude the production of hydrogen gas because we did not observe any bubbles coming from the WE during the whole time of the experiment and the potential for hydrogen evolution is much more negative compared to the one we used in our trial. The ascending trend of current in the runs could be explained by mainly factors:

- the lowering level of medium in the cell and consequent reduction of the area of the electrode exposed to the medium
- the aging and stress of microbial cells:
  - due to the uptake of high current
  - and the lack of any carbon source
- the instability in RE potential is due to:
  - accumulation of cells on the RE porous septum
  - momentarily diminished or total absence of contact between the RE and the medium in the cell due to the growth of biofilm on the RE and the lowering of the medium level in the cell

The lowering level is caused by the constant stream of dry nitrogen gas that passes through the cell and by the sampling of the medium for the quantification of ammonia, while the aging and stress might be due to the accumulation of an

excess of reducing species within the cell [19, 20]. However, this doesn't explain the behavior of the current in runs 8 and 9, which was probably due to the instability in RE potential caused by the intermittent lack of contact with the medium in the cell. This is reflected in the CA of run 8 by the presence of large amount of noise and big spikes which are absent in previous runs.

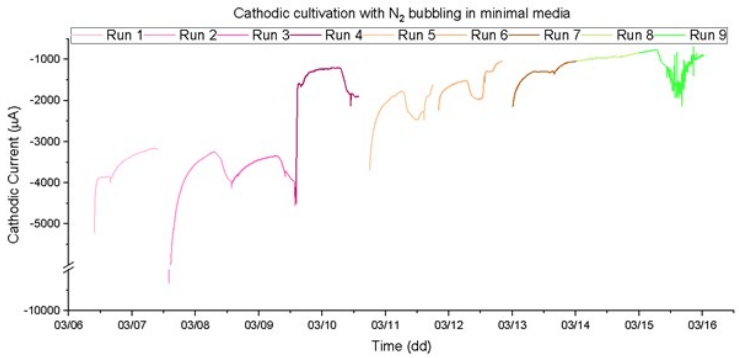

Figure 3.11. Chronoamperometric runs of the nitrogen cultivation experiment, cathodic mode: WE potential poised at $-650\,\mathrm{mV}$ vs Ag/AgCl RE ($\approx -425\,\mathrm{mV}$ vs SHE), each run lasts 24 h.

Figure 3.12 shows that the theoretical production of ammonia in each 24h run within the biofilm corrected for the surface of the immersed electrode closely follows the curve of the current corrected for the immersed electrode, thereby demonstrating the lack of negative effect of the sampling on the current uptake if we exclude the obvious direct effect of current reduction due to the lower exposed area. It also very evident that if we account for this effect, multiplying by the fraction of the full electrode over the immersed electrode area, the activity of the biofilm that is still immersed in the medium is not significantly reduced. However, there is still a visible reduction in current sums during the runs and the possible explanations for this are:

- there was an, even if minimal and momentaneous, oxygen infiltration that may have altered the biofilm metabolism. This could be especially true when sampling with the syringe from the cell since the cell is not pressure proof.
- The rate of ammonia production in the biofilm is far superior to the convection of ammonium ions out of it. Therefore, the consequent accumulation of

ammonium ions in the biofilm has determined a toxic/inhibitory effect on the cell's activity and thus a reduction of the current uptake

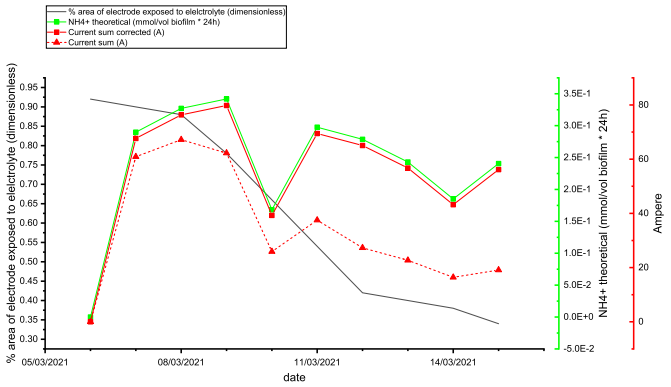

Figure 3.12. This figure shows the comparison between the current sum corrected (red solid curve with square symbol) /non corrected (red dashed curve triangular symbol) for area of immersed electrode (represented by the black curve) and the calculated theoretical concentration within the biofilm on the electrode(green solid curve with square symbols) corrected for the area of the immersed electrode.

The second explanation is supported by the data in figure 3.13 which shows the relation between the ammonium ion concentration measured colorimetrically in the medium samples and the calculated concentration of the same chemical species in the vicinity of the biofilm. In this regard, the red curve, which represents the sum of the production rate of ammonium in the volume of the electrode (within which the diffusion should be slower due to the texture of the electrode and the Extra Cellular Matrix of the biofilm) over 24h (integration of a quantity over time and thus a quantity) shows that at the end of the 9^{th} run the concentration of ammonium is very close to the inhibitory threshold for *Rps. palustris* 42OL of $2.5\,\text{mmol}\,\text{l}^{-1}$.

This could mean that upon the end of the 9 runs, the system formed by the biofilm, the solution in the bulk electrode, and the bulk solution of the cell should have reached an equilibrium that corresponds to the various curves in figure 3.13, in which the red curve represents the concentration in $\text{mmol}\,\text{l}^{-1}$ in the biofilm, the green curve is the concentration of the bulk solution measured colorimetrically, the black is the rate of production per litre and the blue curve is the concentration

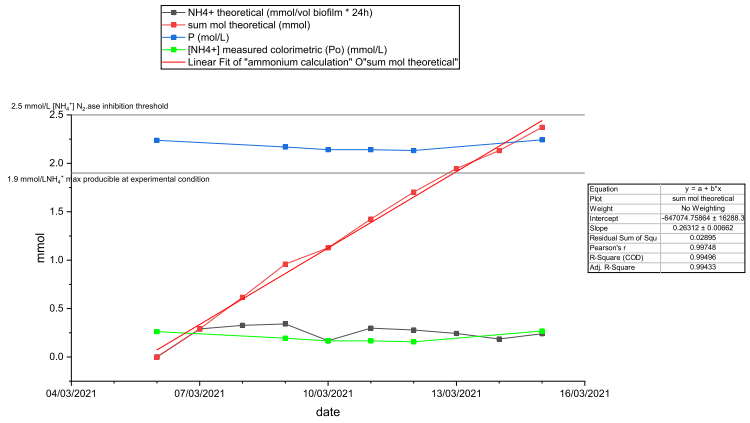

Figure 3.13. Empirical (green) and theoretical (blue, black, red) ammonia concentration curves, from the cathodic cultivation with N_2 bubbling. Green curve represents the trend of ammonia concentration in the bulk medium over time, the black one the theoretical production over the course of each day according to the current passed though the cell within the biofilm, red one is the summation of ammonia the moles produced each day within the biofilm and blue one is the theoretical maximum concentration of ammonia within the biofilm depending on the bulk medium concentration calculated with equation 3.3.2.1

in the biofilm according to equation 3.3.2.1 . Statement that is supported by the tendency toward a plateau of the current curves in figure 3.11.

$$P = \frac{D_{es} \cdot Y_{ps} \cdot S_o}{D_{ep}} + P_o = P_b + P_o \tag{3.3.2.1}$$

Where: P is the theoretical maximal concentration producible in the experimental condition based on diffusion and concentration parameters, calculated according to equation 3.3.2.1 from Stewart in [23]:

- P_b = Limit concentration in biofilm.
- P_o = Concentration of the product bathing in the bulk solution
- D_{es} = Diffusion coefficient of substrate (N_2)
- D_{ep} = Diffusion coefficient of the product (NH_4^+)
- Y_{ps} = Yield coefficient of the reaction
- S_o = Concentration of substrate in the bulk solution

Cyclic voltammetries: evidences of reversible electron transfer pathways

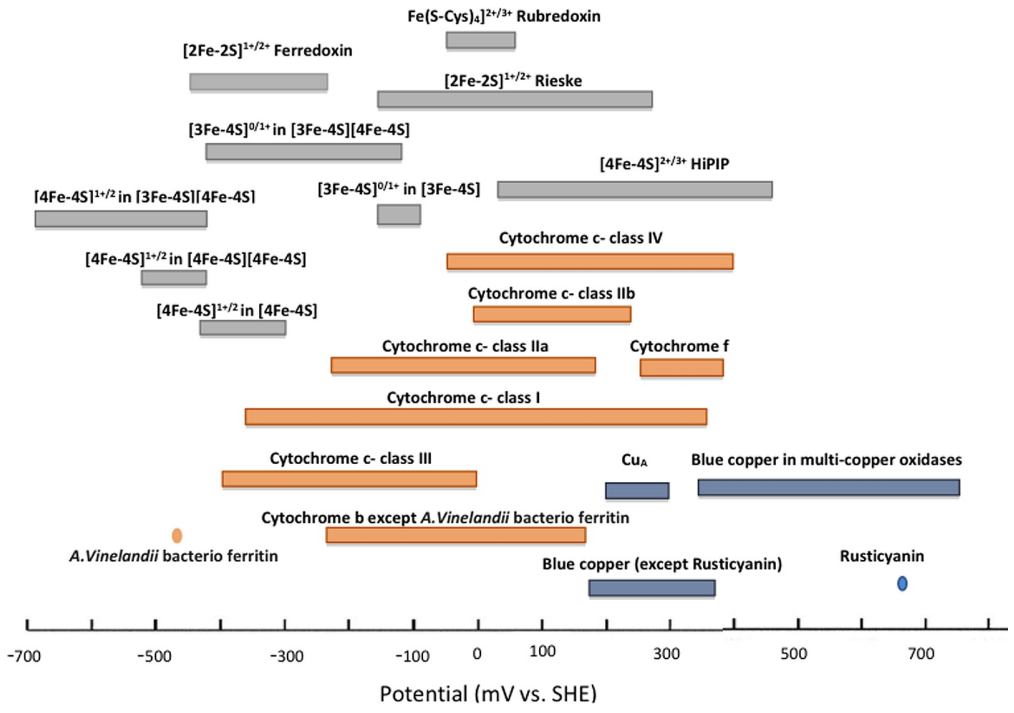

Figure 3.14. The ranges of various E_0 potentials in various types of cofactors belonging to different redox protein classes. Liu et al., Metalloproteins Containing Cytochrome, Iron–Sulfur, or Copper Redox Centers [13].

We performed cyclic voltammetry (CV) analyses in between before run 1, between run 4 and 5 and between run 6 and 7, to shed some light on the electrochemical processes happening on the surface of the colonized electrode. The results show

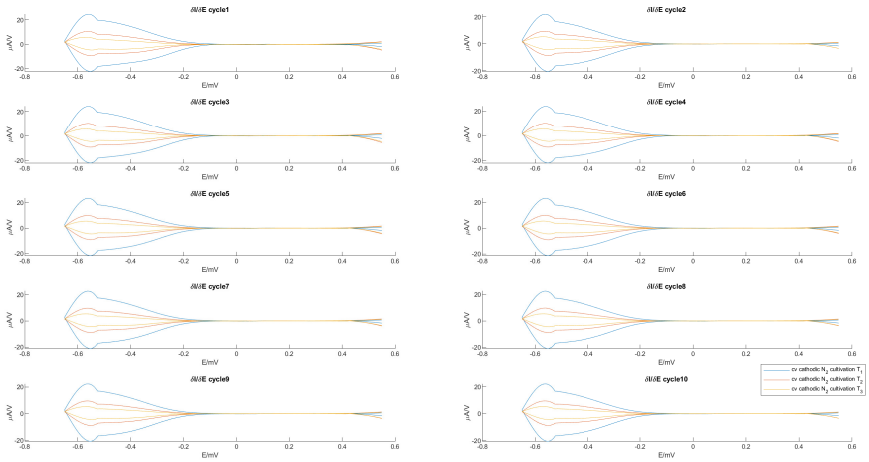

Figure 3.15. Blank-subtracted t_1 to t_3 comparison among cycles of $\Delta I/\Delta E$ over the range of $-650\,\text{mV}$ to $600\,\text{mV}$. Scan rate 5mV/s.

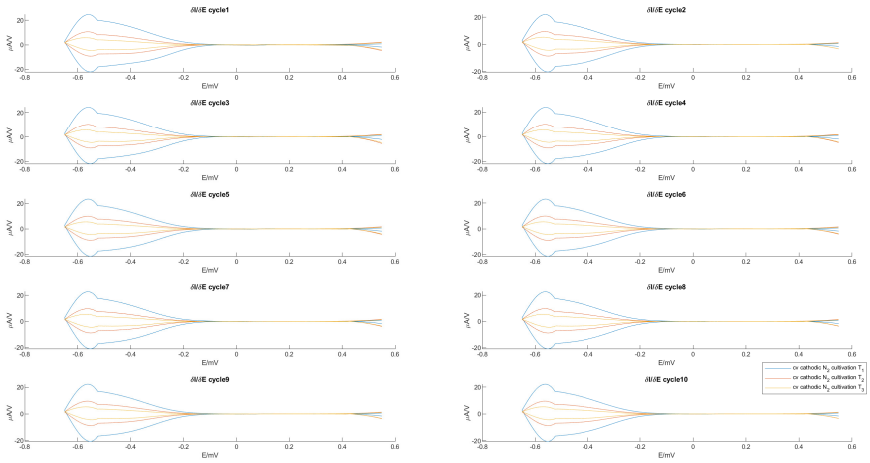

Figure 3.16. Non-blank-subtracted t_1 to t_3 comparison among cycles of $\Delta I/\Delta E$ over the range of $-650\,\text{mV}$ to $600\,\text{mV}$. Scan rate 5mV/s.

clearly enough that aside the expected reduction in the current uptake magnitude due to the lowering media level, there are no permanently evident alterations of the shape of the peaks evidenced through the partial derivation, in respect of the potential, of the current in each scan. This is particularly evident in Figures 3.15 to 3.17 where each set cycle from t_1 to t_3 is plotted in a different quadrant from 1 to

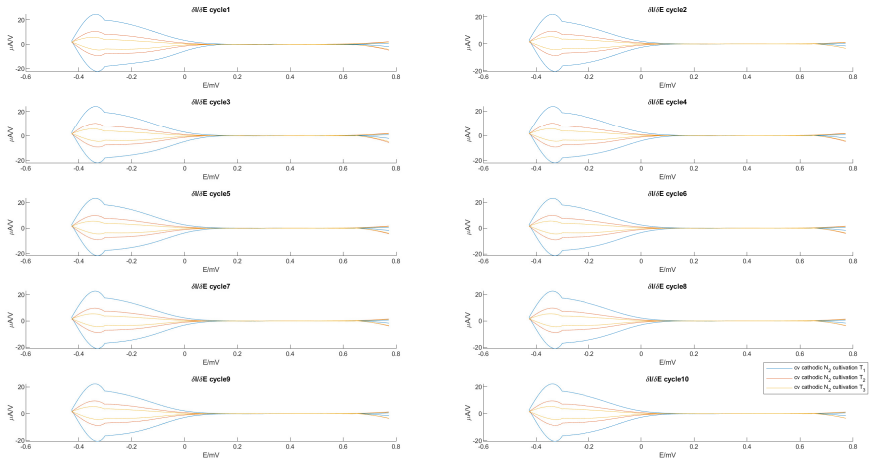

Figure 3.17. Non-blank-subtracted t_1 to t_3 comparison among cycles of $\Delta I/\Delta E$ vs SHE (Standard Hydrogen Electrode) potential scaled range assuming 223 mV as potential of the reference electrode (Ag/AgCl). Scan rate 5mV/s.

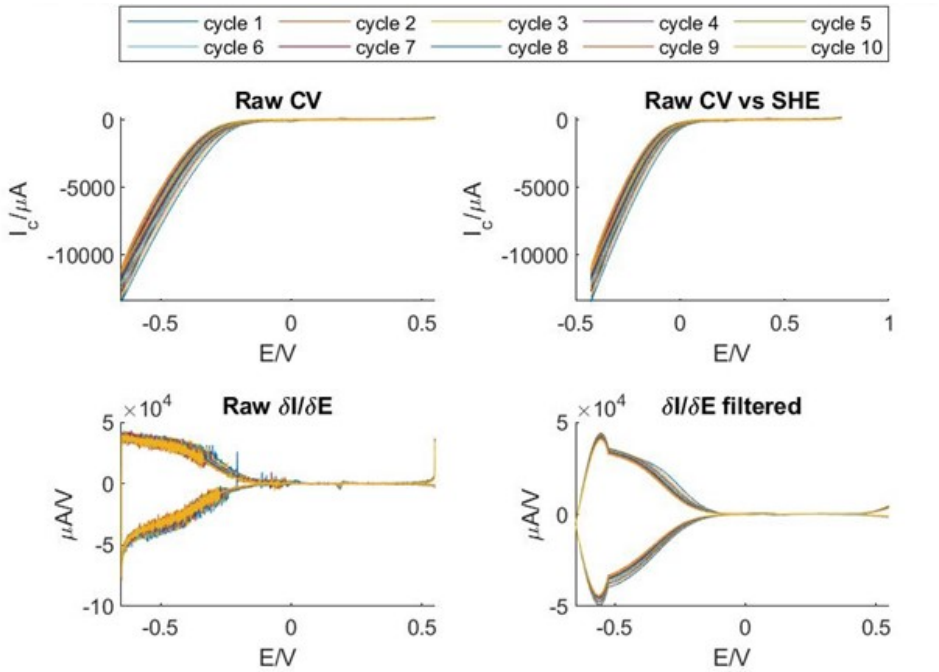

Figure 3.18. Cathodic condition N_2 bubbling at t_1 subtracted of blank scan. Scan rate 5mV/s, scan range −650 mV to 600 mV

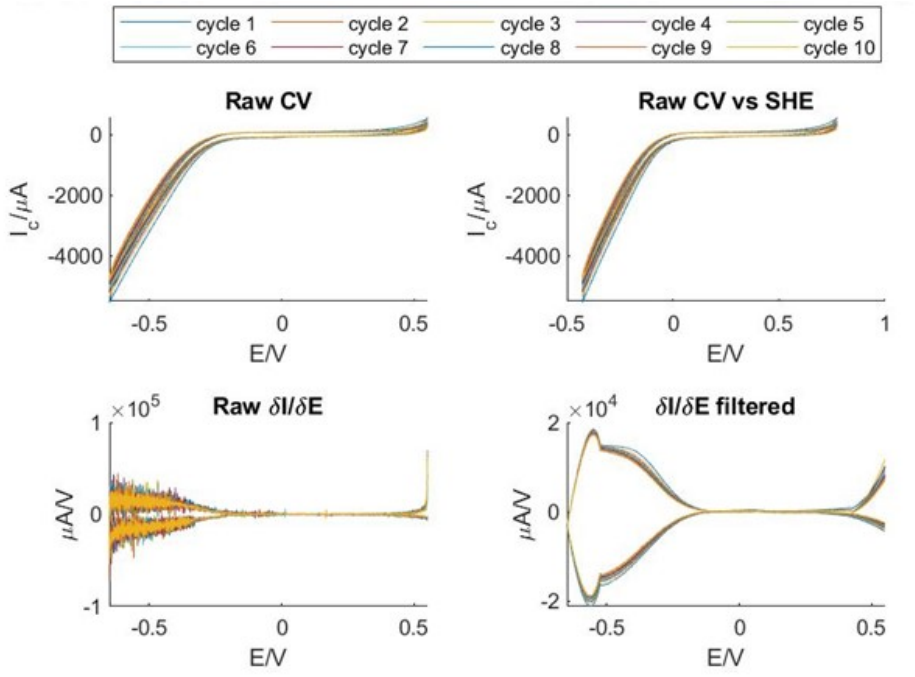

Figure 3.19. Cathodic condition N_2 bubbling at t_2 subtracted of blank scan. Scan rate 5mV/s, scan range $-650\,\text{mV}$ to $600\,\text{mV}$

10 as the number of cycles in each CV.

It should be also noted that the blank scan taken with the abiotic electrode and subtracted from the other experimental readings, does not significantly impact the shape nor the magnitude of the current curves at various scan rates, meaning that there is no hydrogen production and the current is uptaken from the cell with a direct mechanism.

This statement is substantiated by the presence, in the figures 3.15 to 3.17 and in the "δI/δE filtered" quadrant of figures 3.18 to 3.23, of a quasi-symmetric peak around ≈ -380mV vs SHE (≈ -600mV vs Ag$-$AgCl RE) that is in the potential range of 4Fe-4S cluster proteins and class III and possibly class I c-type Cytochromes, as can be seen from figure 3.14 form [13] and of electron uptake machinery known in *Rps. palustris* (see figure 3.1). Another fact against the possibility of catalytic hydrogen production by the electrode is the fact that the potential for HER (Hydrogen Evolution Reaction) on carbon felt is much more negative than the $\approx -427\,\text{mV}$ vs SHE of our most negative potential. There is, however, a current of $\approx -1\,\text{mA}$

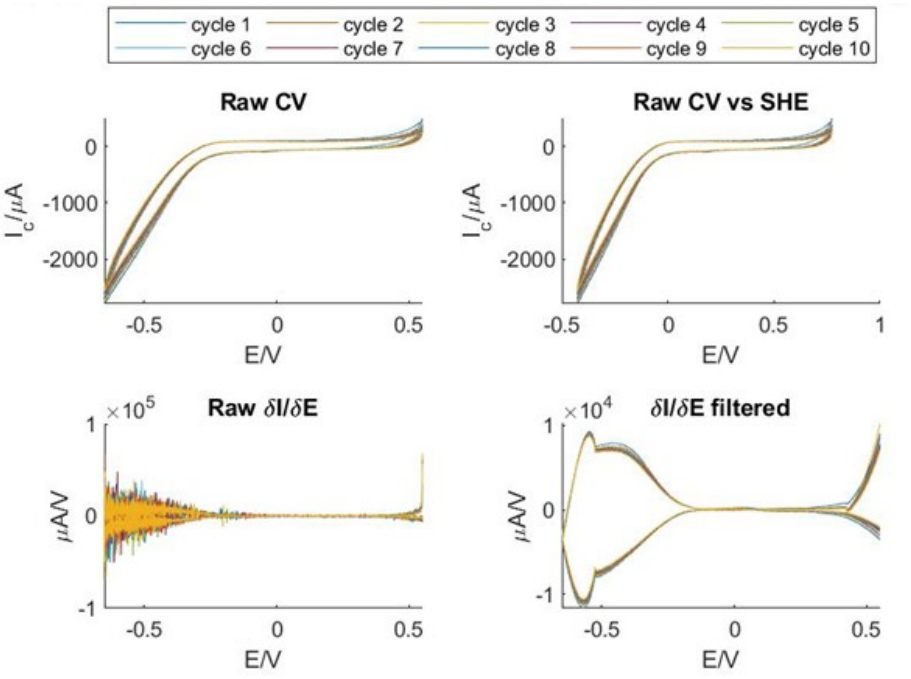

Figure 3.20. Cathodic condition N_2 bubbling at t_3 subtracted of blank scan. Scan rate 5mV/s, scan range −650 mV to 600 mV

at −427 mV vs SHE or −650 mV vs Ag/AgCl in the blank scans, although that could be possibly explained by the electrolytes or other potential metallic impurities in the media or actually by the catalytic activity of the electrode material. It should be noted however, that the current in N_2 reduction condition with inoculated and acclimated biofilm is about 15 times at the same potential, thus meaning that the biological catalytic activity is highly preponderant compared to the one hypothetically due to the pristine electrode.

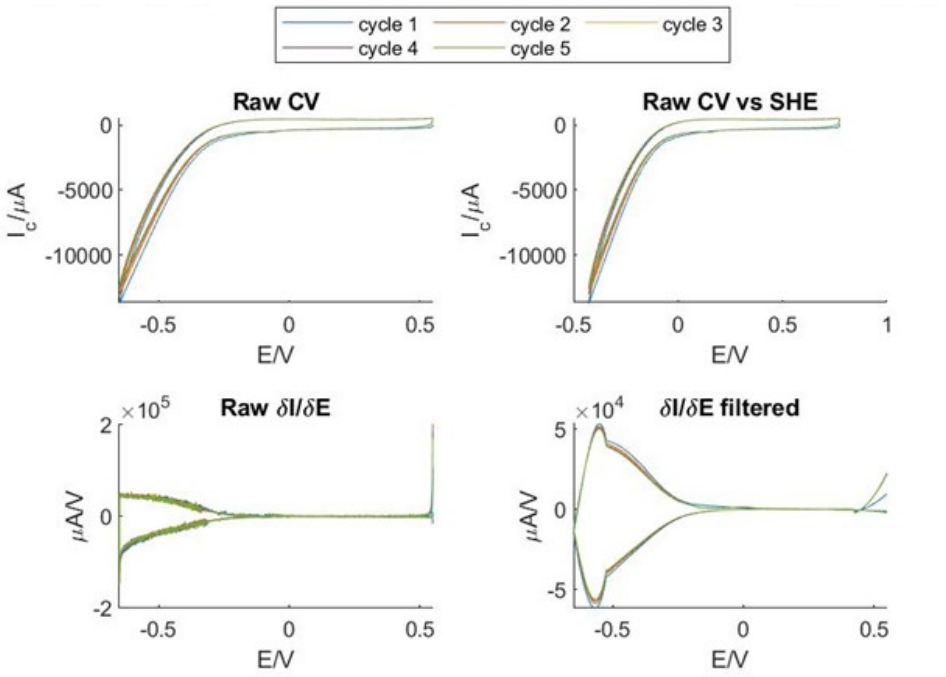

Figure 3.21. Cathodic condition N_2 bubbling at t_1 subtracted of blank scan. Scan rate 50mV/s, scan range $-650\,\text{mV}$ to $600\,\text{mV}$

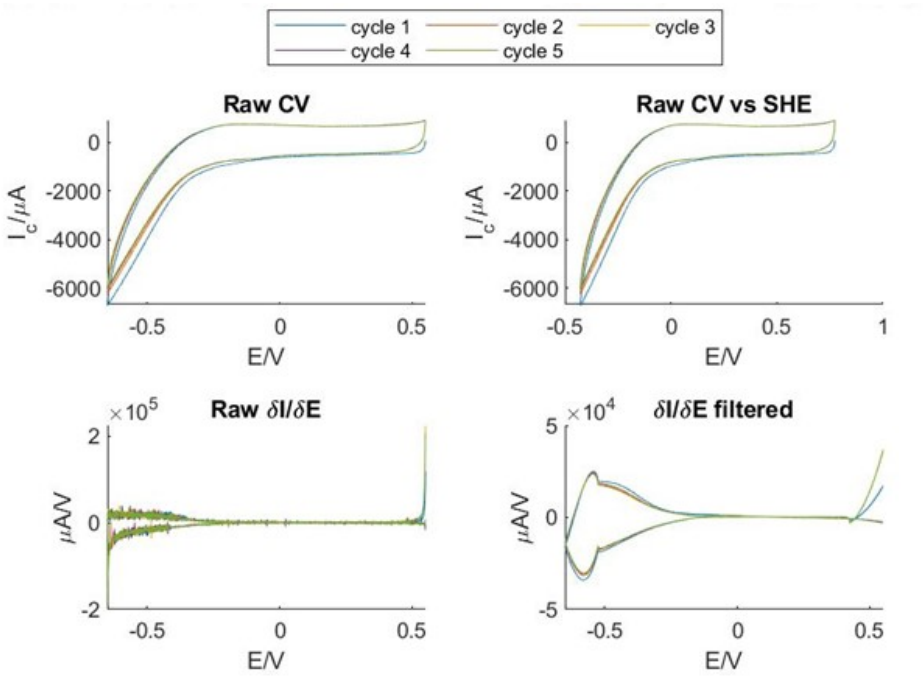

Figure 3.22. Cathodic condition N_2 bubbling at t_2 subtracted of blank scan. Scan rate 50mV/s, scan range −650 mV to 600 mV

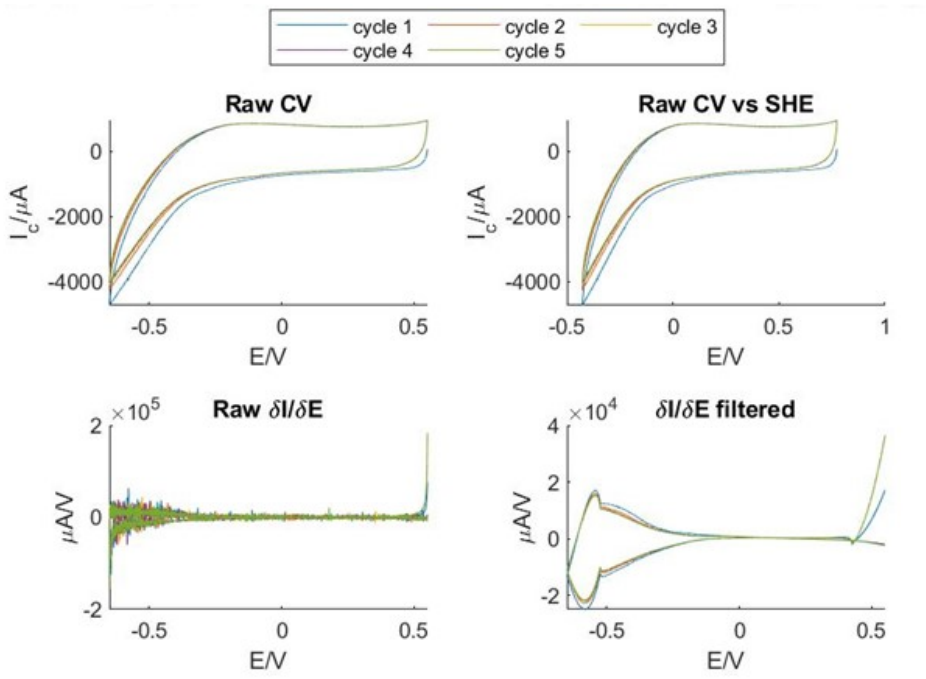

Figure 3.23. Cathodic condition N_2 bubbling at t_3 subtracted of blank scan. Scan rate 50mV/s, scan range $-650\,\text{mV}$ to $600\,\text{mV}$

3.3.3 Supplementary: first clues of circadian rhythm in chronoamperometric measurements

Another detail worth of notice is the presence of a pseudoperiod in almost all chronoamperometric runs throughout the experiment. This is quite surprising and novel discovery that was not reported yet through current measurements in this bacterium. Although it is known in literature [15] that *Rps. palustris* can synchronize its nitrogen fixation patterns with daylight cycles through the expression of KaiCB clock system, it is, to our knowledge, an absolute novelty to find similar temporal patterns in the current uptake of a strain of the same specie.

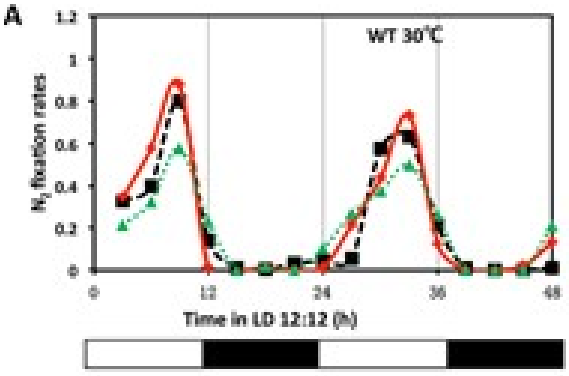

Figure 3.24. A nitrogen fixation activities of the wild-type *Rps. palustris* (WT) at 30°C. The three traces represent three individual cultures under anaerobic conditions that were tested at different phases of LD 12:12 after growth for 2 weeks in LD 12:12. The black and white bars underneath represent the light and dark conditions. Nitrogen fixation rates were calculated based on the amount of C_2H_4 (nmol) produced by 10^{10} cells per hour. These two-cycle LD experiments were repeated twice, each time with 3 replicate cultures. Ma et al. Evolution of KaiC-Dependent Timekeepers: A Proto-circadian Timing Mechanism Confers Adaptive Fitness in the Purple Bacterium Rhodopseudomonas palustris PLOS Genetics, Public Library of Science (PLoS), 2016, 12, e1005922 [15]

As it can be observed from table 3.1 and figure 3.25 below, despite the starting time is significantly different between groups of runs, the inflection point in almost every run occurs at the same time, around 6:30-7:00 am, after which the current

starts to increase until the end of the cycle. This behavior is present despite the fact that the cell is illuminated from below throughout all time of the experiment with a constant power of ≈ 80 watts and therefore, according to Ma et al. should not exhibit any circadian rhythm behavior.

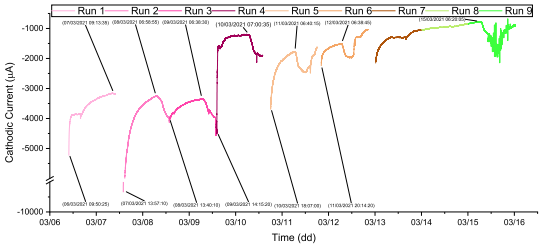

Figure 3.25. Chronoamperometric runs of the nitrogen cultivation experiment, with the approximate inflection points and starting time of each run.

Date	Sunrise time	Inflection point time
07 Sun	06:41:16	09:13
08 Mon	06:39:31	06:58
09 Tue	06:37:46	06:38
10 Wed	06:36:00	07:00
11 Thu	06:34:14	06:40
12 Fri	06:32:28	06:38
13 Sat	06:30:41	
14 Sun	06:28:54	
15 Mon	06:27:07	06:20

Table 3.1. This table list the date and the times of the sunrise and of inflection points in the chronoamperometric curves of the N_2 fixing experiment

Nevertheless, we found out that the time of the flex point in the current roughly corresponds to the time of sunrise in the precise location of the experiment(data from www.sunearthtools.com) for the month (March).

3.4 Discussion

As can be seen, even from the preliminary experiments, the *Rhodopseudomonas palustris* strain 42OL is certainly electrochemically active, like strains TIE-1 [5] and RP2 [24]. These two strains are able to convey, and in some cases uptake, electrons to/from electrodes via Direct Electron Transfer (DET), possibly thanks to the PioABC operon, that is essential for the photoautotrophic growth coupled to iron oxidation, though it is also thought to play an important role in electron exchange with electrodes. Although we could not confirm the involvement of PioABC complex directly, we evidenced how the cells form a dense biofilm on the surface of the electrode fibers via SEM pictures. We could even glimpse the presence of subcellular structures that could be nanowires of some kind connecting cell to cell and cells to the electrode. This is in good accordance with other reports [25] for another strain of the same species, although we cannot conclude that the nanowires are of the same nature.

Another aspect we want to remark is the fact that we could observe significant current uptake from the electrode for nine days straight and the experiment could be continued further if the medium was to be refilled continuously. Nonetheless, this and the result of the ammonium quantitation via colorimetric method constituted sufficient proof to assert that it is very likely that electrochemically driven Biological Nitrogen Fixation (e-BNF) is carried out by *Rps. palustris* strain 42OL at the given experimental condition. Moreover, this would be, to our knowledge, one of the first reports of e-BNF in a single pure culture and could potentially pave the way to commercially viable exploitation. In this regard, the reader should consider that we used an open system with a constant stream of nitrogen and thus the ammonia concentration in the bulk medium was likely to be lower than a closed system could be. Another option that we could not exploit could have been the usage of an ammonia trap to conduct gravimetrical analysis of the ammonium stripped from the medium and the cell's headspace by the flow of nitrogen. However, we can still speculate that the production of ammonia was likely happening in our system at the given experimental conditions.

Although we cannot be certain of this, we believe that we also were able to observe

a new phenomenon of current oscillation in the the last experiment. This oscillation could be ascribed to a molecular clock already reported for *Rhodopseudomonas palustris* in [15] and although not by any means a conclusive proof, a novel example of how it is possible to record the circadian rhythm in electroactive bacteria. The only other report in the literature on this topic is from Lu et al. [14] and it is centered around a cyanobacterium and a *S. elongatus* and a biocompatible electron mediator, poly(2-methacryloyloxyethyl phosphorylcholine-co-vinylferrocene) (Poly(MPC-co-VF); PMF) thus not a direct EET system.

3.5 Conclusions and future directions

In conclusion, we showed that *Rps. palustris* strain 42OL is indeed electrochemically active, in both anodic and cathodic modes. Moreover, that is likely producing extracellular appendages that might serve as electron conducing structures. That it is able to produce a dense biofilm on the electrode fiber surfaces and that is likely to exhibit proto-circadian rhythm. We think our work could have potential relevance especially for the possible applications in e-BNF which are of high interest because of the energy intensive traditional industrial process for ammonia production. Research in this field should become a terrain of interesting discoveries in terms of basic and applied sciences and thus we hope to give with our work a significant contribution to its advancement.

We also evidenced as the electrode construction techniques play an essential role on the current that can be produced by the cells. In this regard, we want to underline the importance of research not only in the biological part of this multidisciplinary subject, but also in the materials and cell construction aspects so that the major problems of these technologies can be overcome and to make them a a commercially viable and perhaps greener alternative to traditional industrial processes.

As a future direction, we plan to reinforce and widen our understanding of the molecular mechanisms by which this strain produces and uptakes currents, and we plan to expand the trials to pure CO_2 and concurrent CO_2 and N_2 mix to verify the feasibility and yield of electrochemically driven PHB and PHAs production.

3.6 Acknowledgement

I hereby thank and acknowledge the CREA-AA and CREA-DC personnel of the site of Cascine del Riccio for invaluable help with the SEM pictures, protocol execution and for the availability of instrumentation and lab space.

References

[1] Alessandra Adessi et al. “Draft genome sequence and overview of the purple non sulfur bacterium Rhodopseudomonas palustris 42OL.” In: *Standards in genomic sciences* 11 (Mar. 2016), p. 24.

[2] Alessandra Adessi et al. “Hydrogen production under salt stress conditions by a freshwater Rhodopseudomonas palustris strain.” In: *Applied Microbiology and Biotechnology* 100.6 (Mar. 2016), pp. 2917–2926.

[3] G. Bertani. “Studies on lysogenesis. I. The mode of phage liberation by lysogenic Escherichia coli”. eng. In: *Journal of Bacteriology* 62.3 (Sept. 1951), pp. 293–300. ISSN: 0021-9193.

[4] Lucia Bianchi et al. “Hydrogen-producing purple non-sulfur bacteria isolated from the trophic lake Averno (Naples, Italy)”. In: *International journal of hydrogen energy* 35.22 (2010), pp. 12216–12223.

[5] A Bose et al. “Electron uptake by iron-oxidizing phototrophic bacteria.” In: *Nature Communications* 5 (Feb. 2014), p. 3391.

[6] Arpita Bose and Dianne K Newman. “Regulation of the phototrophic iron oxidation (pio) genes in Rhodopseudomonas palustris TIE-1 is mediated by the global regulator, FixK.” In: *Molecular Microbiology* 79.1 (Jan. 2011), pp. 63–75.

[7] Marcelo Carmo and Detlef Stolten. “Chapter 4 - Energy Storage Using Hydrogen Produced From Excess Renewable Electricity: Power to Hydrogen”. en. In: ed. by Paulo Emilio V. de Miranda. Academic Press, Jan. 2019, pp. 165–199. ISBN: 9780128142516.

[8] Aisha E. Guardia et al. “Electrochemistry of R. palustris Azul during phototrophic growth”. en. In: *Electrochimica Acta* 355 (Sept. 2020), p. 136757. ISSN: 0013-4686.

[9] Kamrul Hasan et al. “Electrochemical Communication Between Electrodes and Rhodobacter capsulatus Grown in Different Metabolic Modes”. In: *Electroanalysis* 27.1 (Jan. 2015), pp. 118–127. ISSN: 1040-0397.

[10] Kamrul Hasan et al. "Electrochemical communication between heterotrophically grown Rhodobacter capsulatus with electrodes mediated by an osmium redox polymer." In: *Bioelectrochemistry* 93 (Oct. 2013), pp. 30–36.

[11] Dawn E Holmes et al. "The electrically conductive pili of Geobacter species are a recently evolved feature for extracellular electron transfer." In: *Microbial genomics* 2.8 (Aug. 2016), e000072.

[12] Morris J. Karnovsky. "A Formaldehyde-Glutaraldehyde Fixative of High Osmolality for Use in ElectronMicroscopy". In: 1965.

[13] Jing Liu et al. "Metalloproteins Containing Cytochrome, Iron–Sulfur, or Copper Redox Centers". In: *Chemical Reviews* 114.8 (Apr. 2014), pp. 4366–4469. ISSN: 0009-2665.

[14] Yue Lu et al. "Regulation of the Cyanobacterial Circadian Clock by Electrochemically Controlled Extracellular Electron Transfer". en. In: *Angewandte Chemie International Edition* 53.8 (2014), pp. 2208–2211. ISSN: 1521-3773.

[15] Peijun Ma et al. "Evolution of KaiC-Dependent Timekeepers: A Proto-circadian Timing Mechanism Confers Adaptive Fitness in the Purple Bacterium Rhodopseudomonas palustris". In: *PLOS Genetics* 12.3 (Mar. 2016). Ed. by Lotte Søgaard-Andersen, e1005922.

[16] Gion Calzaferri Martin Lanz David SchuÈrch. "Photocatalytic oxidation of water to O and on AgCl-coated and electrodes". In: *Journal of Photochemistry and Photobiology A: Chemistry* (1999).

[17] Dayana Muzziotti et al. "H2 production in Rhodopseudomonas palustris as a way to cope with high light intensities". en. In: *Research in Microbiology* 167.5 (June 2016), pp. 350–356. ISSN: 0923-2508.

[18] Yasuhiro Oda et al. "Functional Genomic Analysis of Three Nitrogenase Isozymes in the Photosynthetic Bacterium Rhodopseudomonas palustris". In: *Journal of Bacteriology* 187.22 (Nov. 2005), pp. 7784–7794.

[19] Jonathan D. Rand and Chris M. Grant. "The Thioredoxin System Protects Ribosomes against Stress-induced Aggregation". In: *Molecular Biology of the Cell* 17.1 (Jan. 2006), pp. 387–401. ISSN: 1059-1524.

[20] Freya Q. Schafer and Garry R. Buettner. “Redox environment of the cell as viewed through the redox state of the glutathione disulfide/glutathione couple”. en. In: *Free Radical Biology and Medicine* 30.11 (June 2001), pp. 1191–1212. ISSN: 0891-5849.

[21] Chuanjun Shu et al. “Direct Extracellular Electron Transfer of the Geobacter sulfurreducens Pili Relevant to Interaromatic Distances.” In: *BioMed research international* 2019 (Nov. 2019), p. 6151587.

[22] Mathangi Soundararajan et al. “Phototrophic N2 and CO2 Fixation Using a Rhodopseudomonas palustris-H2 Mediated Electrochemical System With Infrared Photons”. In: *Frontiers in Microbiology* 10 (2019), p. 1817. ISSN: 1664-302X.

[23] Philip S. Stewart. “Diffusion in Biofilms”. In: *Journal of Bacteriology* 185.5 (Mar. 2003), pp. 1485–1491.

[24] Krishnaveni Venkidusamy and Mallavarapu Megharaj. “A Novel Electrophototrophic Bacterium Rhodopseudomonas palustris Strain RP2, Exhibits Hydrocarbonoclastic Potential in Anaerobic Environments.” In: *Frontiers in microbiology* 7 (July 2016), p. 1071.

[25] Krishnaveni Venkidusamy et al. “Electron transport through electrically conductive nanofilaments in Rhodopseudomonas palustris strain RP2”. In: *RSC Adv.* 5.122 (2015), pp. 100790–100798. ISSN: 2046-2069.

Chapter 4

Work in progress

4.1 Simultaneous selection of soil electroactive bacterial communities associated to anode and cathode in a two-chamber Microbial Fuel Cell

Abstract

Bacteria have evolved strategies to transfer electrons over their cell surface to (or from) their extracellular environment, enabling them to be used in Microbial Fuel Cells (MFCs). Bacterial biocathodes in MFCs represent a potential advantage compared to traditional cathodes, both for their low cost and their low environmental impact. The main challenge in biocathode set-up is to select a bacterial community from an environmental matrix able to accept electrons from the electrode.

A constant voltage was supplied to a two-chamber MFC filled up with soil to select an electron- donor biomass on the anode and an electron-acceptor biomass on the cathode. After three weeks of electrochemical enrichment, total extractable carbon (TEC), humic and fulvic acids (HA+FA), CH_4, CO_2 and N_2O emissions were measured, and bacterial community was analyzed through isolation and high-throughput sequencing techniques.

Results showed that both the experimental conditions and the voltage supply affected soil bacterial communities, providing a selection of different bacteria associated to the anode (Betaproteobacteria, Gracilibacteraceae and Ruminococcaceace) and to

the cathode (Alphaproteobacteria, Clostridium sp. Anaerolinea sp.). An enrichment of Azospirillum and Anaerolinea occurred in the anode. This result is likely related to HA+FA reduction and CO_2 production, as Azospirillum spp. are reported to use HA+FA as electron shuttle. Culturable bacterial community analysis confirmed the differences between anode and cathode, highlighting an enrichment of Solibacillus sp. and Terribacillus sp. in the cathode; phylogenetic analysis on isolated strains revealed a distinction in the species attribution related to the isolation source.
These results confirmed that several potentially electroactive bacteria are naturally present within a top soil and different bacteria could exhibit different electrical properties.

4.2 Bioinformatic analyses and characterization of a novel alkaliphilic electroactive strain's genome and comparison with already characterized related strains

Genome Record

LOCUS	NZ_CP020866 6414964 bp DNA circular CON 21-JUN-2021
DEFINITION	Paenibacillus sp. Cedars chromosome, complete genome.
ACCESSION	NZ_CP020866
VERSION	NZ_CP020866.1
DBLINK	BioProject: PRJNA224116
	BioSample: SAMN06765501
	Assembly: GCF_003184205.1
KEYWORDS	RefSeq.
SOURCE	Paenibacillus sp. Cedars
	Paenibacillus sp. Cedars: Bacteria; Firmicutes; Bacilli; Bacil-
ORGANISM	lales; Paenibacillaceae; Paenibacillus.
REFERENCE 1	(bases 1 to 6414964)
AUTHORS	Hashimoto,K., Okamoto,A. and La Cava,E.

	Genome sequence of Paenibacillus related strain isolated from
TITLE	alkaline pool in The Cedars
JOURNAL	Unpublished
REFERENCE 2	(bases 1 to 6414964)
	Okamoto,A., Rowe,A.R., Yoshimura,M., Nealson,K.H. and La
AUTHORS	Cava,E.
TITLE	Direct Submission
	Submitted (19-APR-2017) Center for Green Research on Energy
	and Environmental Materials, National Institute for Material
	Sciences, National Institute for Material Science, 1 Chome-2-1
JOURNAL	Sengen, Tsukuba, Ibaraki 305-0047, Japan
COMMENT	
REFSEQ	
	The reference sequence is identical to CP020866.1. The annota-
	tion was added by the NCBI Prokaryotic Genome Annotation
	Pipeline (PGAP). Information about PGAP can be found here:
	https://www.ncbi.nlm.nih.gov/genome/annotation_prok/ Bac-
INFORMATION:	teria and source DNA available from Dr. Okamoto Akihiro.

##Genome-Assembly-Data-START##	
Assembly	
Method::	SMRTPortal v. 14-Jan-2016
Assembly	
Name::	SD0178_01_a
Genome	
Representation::	Full
Expected Final	
Version::	No
Genome	
Coverage::	200.0x
Sequencing	
Technology::	PacBio

##Genome-Assembly-Data-END##	
##Genome-Annotation-Data-START##	
Annotation	
Provider::	NCBI RefSeq
Annotation	
Date::	06/21/2021 04:17:28
Annotation	
Pipeline ::	NCBI Prokaryotic Genome Annotation Pipeline (PGAP)
Annotation	
Method ::	Best-placed reference protein set; GeneMarkS-2+
Annotation	
Software	
revision ::	5.2
Features	
Annotated ::	Gene; CDS; rRNA; tRNA; ncRNA;
repeat_region	
Genes (total) ::	6,174
CDSs (total)::	6,070
Genes (coding) ::	5,948
CDSs	
(with protein) ::	5,948
Genes (RNA) ::	104
rRNAs ::	8, 8, 8 (5S, 16S, 23S)
complete	
rRNAs ::	8, 8, 8 (5S, 16S, 23S)
tRNAs ::	76
ncRNAs ::	4
Pseudo Genes	
(total) ::	122
CDSs	

(without	
protein) ::	122
Pseudo Genes	
(ambiguous	0 of 122
residues) ::	
Pseudo Genes	
(frameshifted) ::	75 of 122
Pseudo Genes	
(incomplete) ::	40 of 122
Pseudo Genes	
(internal stop) ::	23 of 122
Pseudo Genes	
(multiple	
problems) ::	15 of 122
##Genome-Annotation-Data-END##	

COMPLETENESS:	full length.
FEATURES:	Location/Qualifiers
	source 1..6414964
	/organism="Paenibacillus sp. Cedars"
	/mol_type="genomic DNA"
	/strain="Cedars"
	/isolation_source="Alkaline pool submerged anode electrode"
	/db_xref="taxon:1980674"
	/country="USA: California, The Cedars, Campsite Springs"
	/lat_lon="38.629472 N 123.122611 W"
	/altitude="269 m"
	/collection_date="2013-09-28"
	/collected_by="Okamoto Akihiro"
CONTIG	join(CP020866.1:1..6414964)